PROBING THE ROLES THAT INTRAFLAGELLAR TRANSPORT B PROTEINS PLAY ON STABILITY, ASSEMBLY, AND LOCALIZATION OF COMPLEX B IN *CHLAMYDOMONAS REINHARDTII*

A Thesis

by

ELIZABETH ANN RICHEY

Submitted to the Office of Graduate Studies of
Texas A&M University
in partial fulfillment of the requirements for the degree of

MASTER OF SCIENCE

Approved by:

Chair of Committee,	Hongmin Qin
Committee Members,	Chaodong Wu
	Lawrence Griffing
Intercollegiate Faculty Chair,	Craig J Coates

December 2012

Major Subject: Genetics

ABSTRACT

Intraflagellar transport (IFT), the key mechanism for ciliogenesis, involves large protein particles moving bi-directionally along the entire ciliary length. IFT particles contain two large protein complexes, A and B, which are constructed with proteins in a core and several peripheral proteins. Prior studies have shown that in *Chlamydomonas reinhardtii*, IFT46, IFT52, and IFT88 directly interact with each other and are in a subcomplex of the IFT B core. However, *ift46*, *bld1*, and *ift88* mutants differ in phenotype as *ift46* mutants are able to form short flagella, while the other two lack flagella completely. In this study, we investigated the functional differences of these individual IFT proteins contributing to complex B assembly, stability, and basal body localization. We found that complex B is completely disrupted in *bld1* mutant, indicating an essential role of IFT52 for complex B core assembly. *Ift46* mutant cells are capable of assembling a relatively intact but highly unstable complex B. In contrast, in *ift88* mutant cells the complex B core still assembles and remains stable, but the peripheral proteins no longer attach to the B core. Moreover, while complex A and the anterograde IFT motor FLA10 are localized normally to the transition fibers, complex B proteins instead are accumulated at the proximal ends of the basal bodies in *ift88*. Taken together, these results revealed a step-wise assembly process for complex B, and showed that the complex first localizes to the proximal end of the centrioles and then translocates onto

the transition fibers via an IFT88-dependent mechanism. Protein interaction analyses such as the yeast two-hybrid assay in addition to identification and characterization of novel IFT complex B mutants will reveal a more complete picture of the architecture and function of IFT complex B.

DEDICATION

To my family for their unconditional love and support; and to all my past teachers and mentors, without whom I would never have made it this far.

ACKNOWLEDGEMENTS

I would like to extend my gratitude to my Principal Investigator and committee chair, Dr. Hongmin Qin, for all her guidance, expertise, and support throughout my graduate career. Her intelligence and experience have been great resources for me during my research. I am grateful for having had the opportunity to be part of her lab.

I also want to thank my committee members, Dr. Chaodong Wu and Dr. Lawrence Griffing, for their support. I appreciate the time they gave to attend committee meetings, sign paperwork, and advise me when necessary.

I would like to acknowledge Elena Lyuksyutova, our lab technician, for preparing media and reagents, maintaining strains, and developing and screening random insertional mutants. Her hard work has made it possible for me to be more efficient and accomplish more from my experiments.

I would also like to thank the other members of the lab for their collaborations, important discussions, and assistance with lab work.

In addition, I acknowledge Jason Brown from the Witman lab for useful information and protocols used for RESDA PCR.

NOMENCLATURE

IFT	Intraflagellar transport
RESDA	Restriction enzyme site-directed amplification
PCR	Polymerase chain reaction
LB	Luria-Bertani (Broth medium)
TAP	Tris-acetate-phosphate medium

TABLE OF CONTENTS

Page

ABSTRACT ii

DEDICATION iv

ACKNOWLEDGEMENTS v

NOMENCLATURE vi

TABLE OF CONTENTS vii

LIST OF FIGURES x

LIST OF TABLES xi

CHAPTER I INTRODUCTION 1

Background 1
Current Knowledge of Complex B……..... 2
Research Objectives and Study Approach…….. 3

CHAPTER II DISSECTING THE SEQUENTIAL ASSEMBLY AND LOCALIZATION OF INTRAFLAGELLAR TRANSPORT PARTICLE COMPLEX B…. 7

Introduction 7
Results……. 8
IFT46 Is Not Essential for Complex B Assembly 8
IFT88 Is Not Essential for Complex B Core Assembly, but is Required for Peripheral Proteins to Attach to the B Core. 11
IFT52 Is Essential for Complex B Core Assembly 11
The Sedimentation Pattern of IFT27 Is Unique from Other Proteins. 12
IFT46 and IFT52 Are Important for IFT Complex B Protein Stabilities, While IFT88 Is Not. 13
IFT Particle Proteins and the Anterograde Motor Fla10 Have Independent Stabilities. 14
IFT52 and IFT88 Are Required for Localization onto the Apical End of the Basal Body…… 17
Discussion…….. 20

Page

Assembly of IFT Complex B Is Sequential and Basal Body Localization Is a Two-step Process 20
IFT88 Is Critical for Mediating the Attachment of Peripheral Proteins to the Complex B Core 22
IFT88 and/or Peripheral Proteins Are Essential for Anchoring Complex B on the Transition Fibers..... 24
The Anterograde Motor Fla10-kinesin-II Must Be Recycled Back to the Cell Body After Each Trip to the Flagellar Tip. 24
Materials and Methods..... 25
Strains and Culture Conditions. 25
Whole Cell Protein Extracts and SDS Page Electrophoresis. 26
Cycloheximide Treatment 26
Western Blotting. 27
Antibodies 27
Sucrose Density Gradient..... 27
Immunofluorescent Staining. 28

CHAPTER III IDENTIFYING INTERACTIONS BETWEEN CORE AND PERIPHERAL PROTEINS..... 29

Introduction… 29
Results and Discussion..... 30
Materials and Methods 31
Strains and Culture Conditions. 31
Plasmids 32
Primer Design..... 32
PCR 33
Cloning and Plasmid Extraction..... 33
Digestions and Ligations 34

CHAPTER IV IDENTIFICATION AND CHARACTERIZATION OF RANDOM INSERTIONAL FLAGELLAR MUTANTS 35

Introduction… 35
Results and Discussion..... 36
Random Insertional Mutagenesis 36
Screening for IFT Mutants 37
RESDA PCR 40
Identification of IFT80, PF16, and CEP290 Mutants 42
Future Aspirations..... 46

Page

Materials and Methods 47
Strains and Culture Conditions 47
Mutagenesis 47
Mutant Screening 48
DNA Extraction 49
RESDA PCR 49
Primers… 51
Sequencing 52

CHAPTER V SUMMARY AND CONCLUSIONS 53

REFERENCES 56

LIST OF FIGURES

Page

Figure 1 Architecture of IFT Complex B in wild type *Chlamydomonas reinhardtii* 2

Figure 2 Phenotypes of wild type, *ift46*, *bld1*, and *ift88* 4

Figure 3 Complex B assembly in *ift46*, *bld1*, and *ift88* mutant cells 10

Figure 4 IFT46 and IFT52 are important for IFT B protein stability, while IFT88 is not 15

Figure 5 IFT protein and motor stabilities are independent from each other 16

Figure 6 IFT88 is required for localization of complex B proteins to transition fibers of basal bodies 18

Figure 7 Complex B proteins localize to the proximal end of the basal bodies in *bld1* 19

Figure 8 Sequential assembly and basal body localization of complex B 23

Figure 9 Multiple insertions or improper digestion of plasmids are common among random insertional mutants made with pHyg3cut with *ScaI* 36

Figure 10 Phototaxis assay 38

Figure 11 Western blot analysis of whole cell extracts revealed potential IFT mutants 39

Figure 12 RESDA PCR 40

Figure 13 A possible *IFT80* mutant is yet to be confirmed 43

Figure 14 10P61 may be a *PF16* mutant 45

LIST OF TABLES

Page

Table 1 Primers Used for Yeast Two-Hybrid Assay 33

Table 2 RESDA Primary PCR Reaction 50

Table 3 RESDA Primary PCR Program 50

Table 4 RESDA Secondary PCR Reaction 51

Table 5 RESDA Secondary PCR Program 51

Table 6 Primers Designed for RESDA PCR 52

CHAPTER I

INTRODUCTION [*]

Background

Cilia and flagella are hair-like organelles extending from the basal bodies of almost all eukaryotic cells. These cellular appendages play important roles for cellular homeostasis and development. Failure to build or maintain functioning cilia leads to a wide spectrum of human diseases and disorders collectively known as ciliopathies, which include hydrocephalus, polycystic kidney disease, primary ciliary dyskinesia, Bardet Biedl Syndrome, etc [1,2].

The assembly and function of the flagella rely on intraflagellar transport (IFT), the conserved bi-directional movement of linear trains of IFT particles along the axoneme [3]. The IFT particle is composed of two complexes, A and B, which play overlapping yet distinct functions for the traffic of IFT. Complex B is essential for the anterograde IFT, while complex A appears to mediate the retrograde movement [4-8]. There are at least 6 subunits in complex A and 13 in complex B [9,10]. In *Chlamydomonas*, both IFT A and B complexes contain a core complex and several peripheral proteins (**Figure 1**). The complex A core refers to the smaller complex found

[*] Reprinted with permission from "Dissecting the Sequential Assembly and Localization of Intraflagellar Transport Particle Complex B in *Chlamydomonas*" by Richey EA, Qin H, 2012. ***PLoS ONE***, 7(8): e43118. doi:10.1371/journal.pone.0043118, Copyright [2012] by Elizabeth Richey.

in a complex A mutant *ift121* [11]. The complex B core is an 11S complex that stays intact in high ionic conditions [12].

Current Knowledge of IFT Complex B

Using the *E. coli* co-expression system, previous studies have revealed that the complex B core contains at least two tetrameric subcomplexes IFT81/74/27/25 and IFT88/70/52/46 [13]. IFT52 was suggested to bridge the two tetramers since it directly interacts with IFT81/74/27/25 [13]. IFT27/25 and IFT81/74 form two stable dimer complexes [12,14,15]. The IFT88/70/52/46 tetramer contains many strong interactions. IFT52, IFT46, and IFT88 interact with each other [13,16], while IFT52 and IFT46 also interact with IFT70 [13,17]. Pair-wise interaction assays have provided some detailed information as to the structure of the complex B core. However, little is known as to how the interactions among the subcomplexes contribute to the in vivo assembly of the functional complex B.

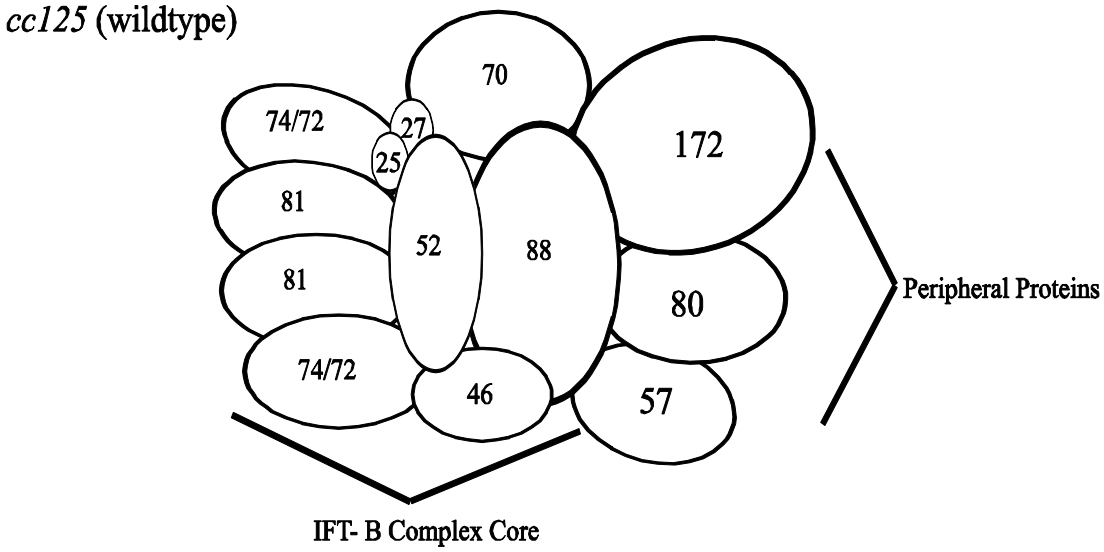

Figure 1. Architecture of IFT Complex B in wild type *Chlamydomonas reinhardtii.*

To date, many IFT protein mutants have been identified in various organisms. These mutants all have defects in ciliogenesis. However, the severity of such defects varies among the mutants. For example, in *Caenorhabditis elegans*, the cilia of *osm-6/ift52* and *osm-5/ift88* mutants are highly stunted with no ciliary axonemal microtubules beyond the transition zone [18]. In contrast, *dyf-6/ift46* [19], *dyf-1/ift70* [20], *ift74*, and *ift81* [21,22] mutants are capable of assembling the middle segment of the chemosensory amphid and phasmid cilia, and IFT motility is intact in the remaining cilia. So far, the function of IFT88 has been studied in many different species. The IFT88 mutants of *Chlamydomonas* [23], *Drosophila* [24], and mouse [25] are all incapable of assembling cilia, demonstrating that IFT88 plays an essential and conserved role in ciliogenesis. The *Chlamydomonas* mutant of IFT52, *bld1*, is completely flagella-less [26], which is consistent with the phenotype seen in *C. elegans*. The *Chlamydomonas ift46* mutant [27] and the *Tetrahymena dyf-1/ift70* [28] mutant have very short flagella with severely disrupted axonemal structures. The fact that neither *dyf-6/ift46* nor *dyf-1/ift70* are completely flagella-less indicates IFT46 and IFT70 do not completely abrogate IFT and ciliogenesis.

Research Objectives and Study Approach

Chlamydomonas IFT46, IFT52 and IFT88 are in the same subcomplex of the IFT B core and can form a stable trimetric complex [16]. Multiple interactions have been found among these three subunits, thus it was expected that deletion of any of the components would destroy the entire complex, and stop IFT. However, their mutants differ in phenotype as *ift46* mutants are able to form short flagella [27], while the other

two mutants lack flagella completely [23,26] (**Figure 2**). This led us to ask, what are the different roles that IFT46, IFT52, and IFT88 play in IFT, and how can these differences

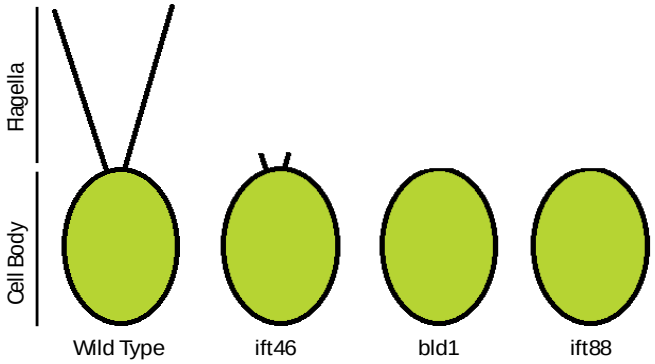

Figure 2. Phenotypes of wild type, *ift46*, *bld1*, and *ift88*. Compared to wild type, *ift46* is able to produce stumpy flagella, while *bld1* and *ift88* are unable to produce flagella.

lead to presence or absence of flagella in these mutants? To answer these questions, the research objectives are as follows:

1. Determine the assembly status of complex B in *ift46*, *bld1*, and *ift88* mutants. Sucrose density gradients were utilized to identify which proteins cosedimented, and therefore were likely to be in complex with each other. This made it possible to conclude the level of complex B disruption in each mutant, leading to a more clear understanding of how IFTs 46, 52, and 88 are important in complex B assembly.

2. Analyze stability of IFT and motor proteins in *ift46*, *bld1*, and *ift88* mutants. Cell cultures were treated with cycloheximide, a protein synthesis inhibitor, and samples were taken throughout a time course. This assay demonstrated the relationships between

IFTs 46, 52, and 88 with the stabilities and turnover rates of other IFT and motor proteins.

3. Identify the localization patterns of IFT proteins in *ift46*, *bld1*, and *ift88* mutants. Immunofluorescent staining revealed the importance of IFTs 46, 52, and 88 in the proper localization of IFT particles to the initiation site for ciliogenesis.

4. Detect interactions between core and peripheral proteins. Yeast two-hybrid assays [29] will be used to determine which IFT proteins can bind with each other. This will allow us to unravel the mystery of how the peripheral proteins and the core proteins interact to form a functional complex B and will unveil the architecture of the complex B periphery.

5. Isolate and characterize random insertional flagellar mutants. Random insertional mutants were screened for phototaxis negativity and flagellar dysfunction or abnormalities. Restriction enzyme site-directed amplification (RESDA) [30] was used to identify which genes were disrupted. Further analysis of IFT-related mutants will reveal a more complete picture of the structure of complex B and the functions of the individual IFT B proteins as they work together as a unit.

By analyzing the *Chlamydomonas* mutants, we concluded that *ift46* is able to form short flagella because it still forms a functional, yet unstable, complex B. Although *ift88* maintains IFT protein stabilities and forms the complex B core, its inability to localize the complex B to the initiation site for ciliogenesis may account for its failure to assemble flagella. The *bld1* mutant has decreased IFT stabilities, a disrupted complex B core, and a failure to localize complex B proteins to the transition fibers of the basal

bodies, all of these factors leading to a flagella-less phenotype. These results provided insight into the in vivo assembly process of complex B and revealed for the first time that IFT complex B first localizes to the proximal end of the centrioles and then translocates onto the transition fibers via an IFT88-dependent mechanism. Results from yeast two-hybrid assays and identification and characterization of novel IFT mutants will also increase our understanding of the IFT process and the assembly and structure of IFT complex B.

CHAPTER II

DISSECTING THE SEQUENTIAL ASSEMBLY AND LOCALIZATION OF INTRAFLAGELLAR TRANSPORT PARTICLE COMPLEX B [*]

Introduction

Complex B is made up of peripheral proteins and a core (**Figure 1**) which can be further divided into at least three smaller subcomplexes: IFT27/25, IFT88/70/52/46, and IFT81/74 [11-15]. IFT52 is thought to be the bridge between these three subcomplexes [13]. The specific purposes of and interactions between each of the IFT B proteins are not completely understood. Even though IFTs 46, 52, and 88 are members of the same subcomplex B [13,16], they may serve different functions for ciliogenesis. This is evident when characterizing the phenotypes of null mutants. *Chlamydomonas reinhardtii* *ift88* [17] and *bld1* [18] (an IFT52 null mutant) have completely flagella-less phenotypes, while *ift46* [19] is able to produce short flagella (**Figure 2**). Therefore, IFT52 and IFT88 are required for ciliogenesis, while IFT46 is not, signifying different roles for these three IFT B core proteins. Here we seek to understand the functional differences between these three proteins in the complex B core by analyzing the

stability, localization, and status of assembly of the complex B core in *ift46*, *bld1*, and *ift88* mutants.

Results

IFT46 Is Not Essential for Complex B Assembly

Sucrose density gradients were used to investigate the assembly status of IFT complex B in *ift46, ift88*, and *bld1/ift52* mutants (**Fig. 3**). In wild type (**Fig. 3A)**, all probed complex B core proteins cosedimented at about 15S, representing the preassembled complex B. Consistent with previous findings [7,9,31], IFT172, a peripheral B protein, peaked at about 13S, confirming that this peripheral protein can readily dissociate from complex B without disrupting the structure of the complex.

IFT B proteins from *ift46* mutant showed a very similar sedimentation pattern to wild type (**Fig. 3B**). Like wild type, all the IFT B proteins peaked at about 15S. However, IFT52 had an additional peak at about 11S, indicating that this protein exists in two separate complex forms. The 11S complex likely serves as an intermediate transition complex, while the 15S complex is a completely or almost completely assembled complex B. IFT74 and IFT81, however, were only found at the 15S peak together with IFT52 and there were no free IFT74 and IFT81 proteins. There was a dramatic increase in the amount of 6S IFT27/25, indicating that a significant fraction of IFT27/25 freely exists. Based on these results, we concluded that IFT46 is not required for assembly of the IFT complex B. Since short flagella do form in *ift46* mutant [27], the 15S complex B is likely functional and capable to support flagellar assembly.

When co-expressed in *E. coli*, complex B proteins assemble into several subcomplexes including two tetrameric subcomplexes, IFT81/74/27/25 and IFT88/70/52/46, and two dimer complexes, IFT27/25 and IFT81/74 [12-14,32]. The *ift46* mutant contained the 15S complex B, an 11S transitional complex, and a free IFT27/25 complex (**Fig. 3B**). IFT52, IFT25, and IFT27 were found in the 11S complex, thus the 11S complex likely is comprised of IFT88/70/52/27/25. Interestingly, IFT81 and IFT74 were only detected in the 15S complex, with no free IFT81/74 complex. Therefore, unlike IFT27/25 subcomplex, the IFT81/74 complex does not exist independently. This result is consistent with previous findings that the full length IFT81/74 expressed in *E. coli* is insoluble [13]. The IFT81/74 complex may not be stable without being bound to the complex B core proteins and thus quickly degrades *in vivo*. Taken together, these results showed that the complex B core appears to assemble in a sequential order: the IFT88/70/52/46/27/25 subcomplex would have to form first in order to allow IFT81/74 to assemble onto the core.

In the *ift46* mutant, complex B proteins still assembled into the 15S complex, which clearly showed that IFT46 is not required for assembly of the IFT complex B. However, without IFT46 the efficiency for assembly is reduced, which allows the accumulation of the 11S intermediate transitional complex (**Fig. 3B**). IFT46 is likely assisting in the efficient binding of the subcomplexes IFT81/74 and IFT88/70/52/46/27/25 to form the complex B core.

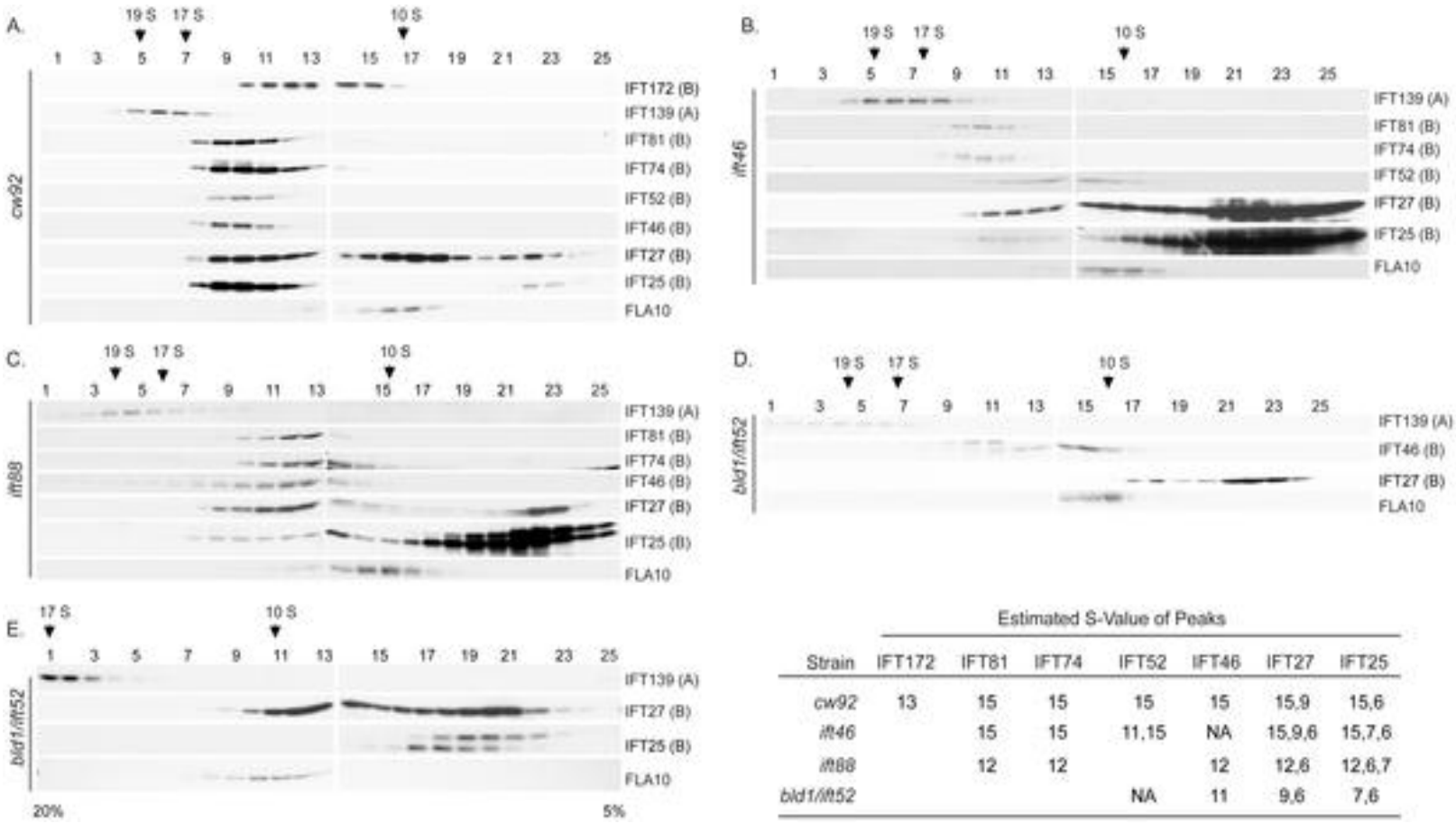

	Estimated S-Value of Peaks						
Strain	IFT172	IFT81	IFT74	IFT52	IFT46	IFT27	IFT25
cw92	13	15	15	15	15	15,9	15,6
ift46		15	15	11,15	NA	15,9,6	15,7,6
ift88		12	12		12	12,6	12,6,7
bld1/ift52				NA	11	9,6	7,6

Figure 3. Complex B assembly in *ift46*, *bld1*, and *ift88* mutant cells. 10–25% sucrose gradients were used for all strains, along with one 5–20% gradient for *bld1*. (A) *cw92*, a cell wall defective mutant which has wild type IFT particles, was used as the control. IFT complex B sedimented at about 15 S. IFT27 had additional peaks at 9 S and 6 S. IFT25 had an additional peak at 6 S. IFT172 peaked at about 13 S. (B) *ift46* mutant still assembled a nearly complete complex B. IFT52 had an additional peak at 11 S. Also, a high concentration of IFT25 and IFT27 was found to peak at S-values as low as 6 S. There was an additional peak for IFT27 at about 9 S. (C) *ift88* mutant had a 12 S complex. Also note that like *ift46*, this strain had a large amount of IFT25 and IFT27 that peaked as low as 6 S, however lacked the 9 S peak for IFT27. (D, E) In *bld1* mutant, IFT46 peaked at approximately 11 S and IFT25 and IFT27 peaked at 6 S. IFT27 had an additional peak at 9 S. No other B proteins were detected due to low amounts of IFT B proteins in *bld1*.

IFT88 Is Not Essential for Complex B Core Assembly, but is Required for Peripheral Proteins to Attach to the B Core

In *ift88* mutant cells, complex B proteins formed a small complex sedimenting at about 12S (**Fig. 3C**) [33], indicating the complex B core is still intact, but at least some peripheral proteins fail to assemble onto the core. Therefore, IFT88 is not required for IFT complex B core assembly, but rather bridges peripheral proteins to the core.

IFT52 Is Essential for Complex B Core Assembly

Previous pair-wise interaction studies have shown that IFT52 binds directly to the IFT81/74/27/25 complex [13], which leads to the possibility that IFT52 serves as a bridge to connect the two tetrameric complexes, IFT88/70/52/46 and IFT81/74/27/25, to form the complex B core. However, it is unclear whether association of these two tetramers solely depends on IFT52. Unlike the *ift46* and *ift88* mutants, the *bld1* cells showed a much disrupted complex B (**Fig. 3D, E**). Since this mutant had extremely reduced amounts of IFT proteins (**Fig. 4A**), we were only able to detect IFT46, IFT25, and IFT27 on the gradients. IFT46 peaked at about 11S. This 11S complex likely contained IFT88, IFT70, and IFT46. Interestingly, unlike the 11S intermediate transition complex found in the *ift46* mutant (**Fig. 3B**), IFT25 and IFT27 were not detected in the 11S fractions in the *bld1* mutant (**Fig. 3D, E**). Therefore, the 11S complex of *bld1* was only composed of the IFT88/70/46 subcomplex, but not IFT27/25. The intermediate transition complexes, IFT27/25 and IFT88/70/46, stayed as two separate subcomplexes that failed to assemble into the complex B core in the *bld1* mutant. Based on the results from the *ift46* and *bld1* mutant gradients, we concluded that IFT52, but not IFT46, is

essential for the binding of IFT88/70/52/46 and IFT27/25. During complex B core assembly, IFT88/70/52/46 and IFT27/25 must assemble into the complex IFT88/70/52/46/27/25 to allow the subsequent binding of IFT81/74.

The Sedimentation Pattern of IFT27 Is Unique from Other Proteins

Unexpectedly, IFT27 formed at least three peaks in wild type (**Fig. 3A**), which is different from what we have observed previously [14]. Prior studies show that IFT27 forms two peaks, one with complex B, and the other in the dimer complex IFT27/25. The third complex that we observed sedimented at approximately 9S. The IFT B proteins that we probed did not cosediment at 9S, thus this 9S complex contained IFT27 bound to other unknown proteins. The 9S complex was observed not only in wild type, but also in *ift46* and *bld1* mutant cells (**Fig 3B, C** and **D**). However, the 9S complex was not observed in *ift88*. One possible explanation to this phenomenon is that in wild type, *bld1*, and *ift46* mutants, IFT27 forms a subcomplex with one or a group of the peripheral proteins, whereas it is unable to do so in the *ift88* mutant since IFT88 may be required to recruit these peripheral proteins and allow binding to IFT27. Checking the sedimentation patterns of peripheral proteins to see if they peak with the 9S IFT27 subcomplex will allow us to test this idea.

IFT25 is a highly phosphorylated protein. The higher molecular weight band represents the phosphorylated form since it migrates slower on the gel [14]. The phosphorylated and the non-phosphorylated IFT25 were readily separated on the *ift88* and *bld1* gradients (**Fig. 3C, D** and **E**). Interestingly, IFT27 cosedimented with the phosphorylated form of IFT25 at approximately 6S, but not with the non-phosphorylated

form. These results hinted that the phosphorylation of IFT25 regulates the binding between IFT27 and IFT25.

IFT46 and IFT52 Are Important for IFT Complex B Protein Stabilities, While IFT88 Is Not

Based on western blot analysis of whole cell protein extracts (**Fig. 4A**), the mutants *ift46*, *bld1*, and *ift88* all showed greatly reduced amounts of complex B proteins when compared to wild type cells. IFT25 was an exception and followed a similar pattern to IFT A rather than B proteins. This may be because IFT27/25 subcomplex is stable apart from the core complex and therefore if IFT B proteins are reduced, it is not affected as the other B proteins. Complex A proteins were not reduced but rather were either increased, as in *ift46* and *ift88*, or remained constant, as in *bld1*. This is consistent with previous findings that complex B mutants often have overexpressed complex A proteins and under-expressed complex B proteins [17,23,27,34]. Of the three mutants, *bld1* had the greatest reduction in complex B proteins, suggesting that IFT52 is extremely important for maintaining cellular levels of complex B proteins. IFT46 and IFT88 are also very important for maintaining cellular levels, but to a lesser extent than IFT52.

A cycloheximide treatment time-course experiment was conducted to measure the degradation and turnover rates of IFT proteins in these mutants. IFT proteins were very stable in wild type cells with no noticeable degradation within 16 hours of treatment (**Fig. 4B**). The *ift88* mutant cells showed a slight decrease but near wild type stabilities of IFT proteins (**Fig. 4C**). In contrast, except IFT25 and IFT27 (data not

shown), *ift46*, and *bld1* cells had an extreme decrease in IFT B protein stabilities, with a dramatic drop in the amount of IFT B proteins within 4 hours of treatment (**Fig. 4D, E**). Thus IFT46 and IFT52 are important for preventing degradation of IFT complex B proteins.

IFT Particle Proteins and the Anterograde Motor Fla10 Have Independent Stabilities

To understand whether the defective complex B affects the expression of the anterograde IFT motor Fla10, the whole-cell amount of FLA10, a subunit of the Fla10 motor, was tested in *ift46*, *bld1*, and *ift88* mutants. FLA10 appeared either at the same level or slightly higher than that of wild type (**Fig. 5A**). A cycloheximide time-course treatment showed that FLA10 was very stable in wild type cells, and in *ift46*, *bld1*, and *ift88* mutants (**Fig. 5B)**. Thus, the reduced amounts of complex B proteins (**Fig. 4A**) or reduced stabilities of B proteins (**Fig. 4D, E**), do not affect the stability of FLA10.

A reciprocal cycloheximide time-course treatment experiment of *fla10*, a null mutant of a FLA10 allele, was carried out to examine if the lack of FLA10 affects the stabilities of complex A or B proteins. Throughout the 16 hour cycloheximide treatment there was no reduction in IFT proteins (**Fig. 5C**). Taken together, these results demonstrated that the stability of IFT particle proteins and the anterograde motor Fla10 are regulated through independent mechanisms.

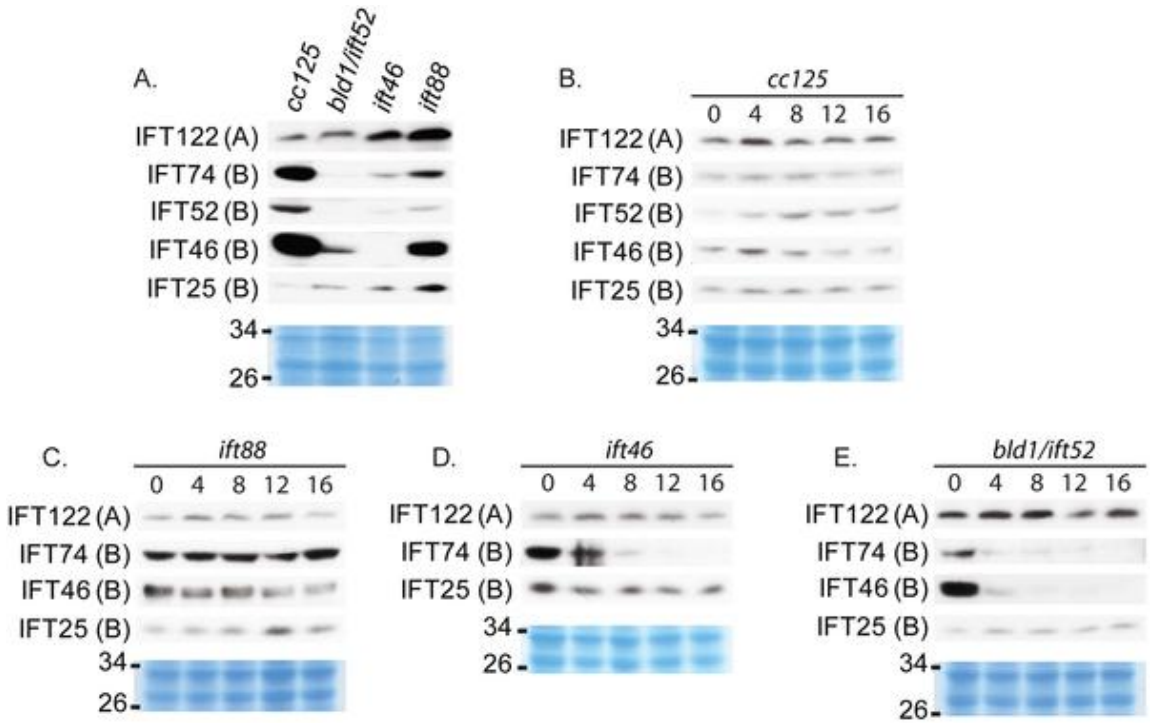

Figure 4. IFT46 and IFT52 are important for IFT B protein stability, while IFT88 is not. Western blot analysis of whole cell extracts of untreated strains or strains treated with cycloheximide. Coomassie-stained gels (in blue color) were used to show equal protein loadings. (A) *Bld1*, *ift46*, and *ift88* have different levels of reduction of IFT B proteins, and an increase or no change in IFT A proteins; *Bld1* shows the most extreme change, while *ift88* shows the least extreme change compared to wild type. (B–E) Cells were treated with cycloheximide, a protein synthesis inhibitor, to measure degradation rates of existing proteins within 16 hours of treatment. (B) In wild type (*cc125*) IFT A and IFT B proteins remain stable throughout the time course. (C) *Ift88* has near wild type stabilities of IFT A and IFT B proteins. (D) *Ift46* has stabilities much like *bld1* for IFT A and IFT B proteins. (E) *Bld1* has an extreme decrease in IFT B protein stabilities, with the exception of IFT25, and no change in stability of IFT A proteins.

The anterograde motor Fla10 is a heterodimer kinesin-II, containing two motor subunits FLA10 and FLA8, and an associated protein FLA3 [35]. *Fla10*^{ts} and *fla3-1b* are two temperature sensitive (ts) mutants of the subunit FLA10 [36] and FLA3 [37], respectively. At the permissive temperature, the mutant proteins FLA10 and FLA3 are capable of supporting the flagella assembly and maintenance, but are inactivated at the non-permissive temperature, leading to the loss of flagella [9,36-38]. We found that at the permissive temperature, when these two mutants were treated with cycloheximide, FLA10 greatly reduced in amount within four hours of the treatment in both mutants

(**Fig. 5D, E**), indicating that the FLA10 protein is highly unstable and has a quick turnover rate. Since not only the *fla10*^{ts}, but also the *fla3-1b* mutant, had reduced stabilities of FLA10, it is likely that each subunit contributes to the stability of the heterodimer Fla10-kinesin-II complex. Reduced stability of a single Fla10-kinesin-II complex protein causes higher turnover rate of the entire complex.

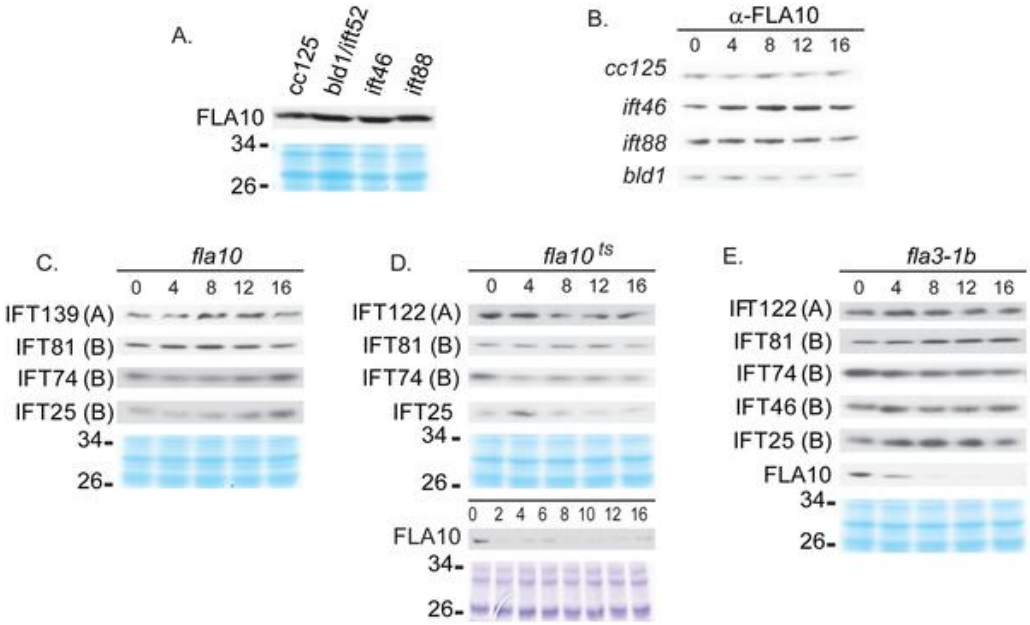

Figure 5. IFT protein and motor stabilities are independent from each other. Western blot analysis of whole cell extracts of untreated strains or strains treated with cycloheximide. Coomassie-stained gels (in blue color) were used to show equal protein loadings. (A) Untreated cells of *ift46*, *ift88*, and *bld1* had the same or slightly higher amount of FLA10 compared to wild type *cc125*. (B) The FLA10 protein was stable throughout 16 hrs of cycloheximide treatment in the wild type cells as well as in the mutants *ift46*, *ift88*, and *bld1*. (C–E) IFT A and B proteins were stable in *fla10* null (C), *fla10*^{ts} (D), and *fla3-1b* (E) mutants throughout the cycloheximide treatment.

IFT52 and IFT88 Are Required for Localization onto the Apical End of the Basal Body

It is perplexing that although the complex B core is intact, the *ift88* mutant is completely flagella-less. We reasoned that the failure to assemble flagella could be due to mislocalization of IFT particle proteins. In wild type cells, IFT particle proteins localize to transition fibers that extend from the distal portion of the basal body to the cell membrane [38] (**Fig. 6A**). The side view of the staining of IFT particle proteins and FLA10 is seen as a band beneath each flagellum ([9,27,38] also see **Fig. 6B**). Similar to wild type, IFT139 (an IFT A protein) colocalized with FLA10 onto the basal bodies in the *ift88* mutant cells (**Fig. 6C**). Interestingly, in *ift88* mutant, FLA10 not only was seen as two bands at the apical end of the cell, but also appeared to extend further beyond the transition fibers and appeared to cover the entire transition zone (**Fig. 6C** arrows). In contrast, IFT139 was only observed as two bands at the transition fibers. The same localization patterns were also observed in *bld1* mutant (**Fig. 7,** arrows). These results indicated that the anterograde motor FLA10-kinesin-II could enter the flagellar compartment without attaching to IFT particles.

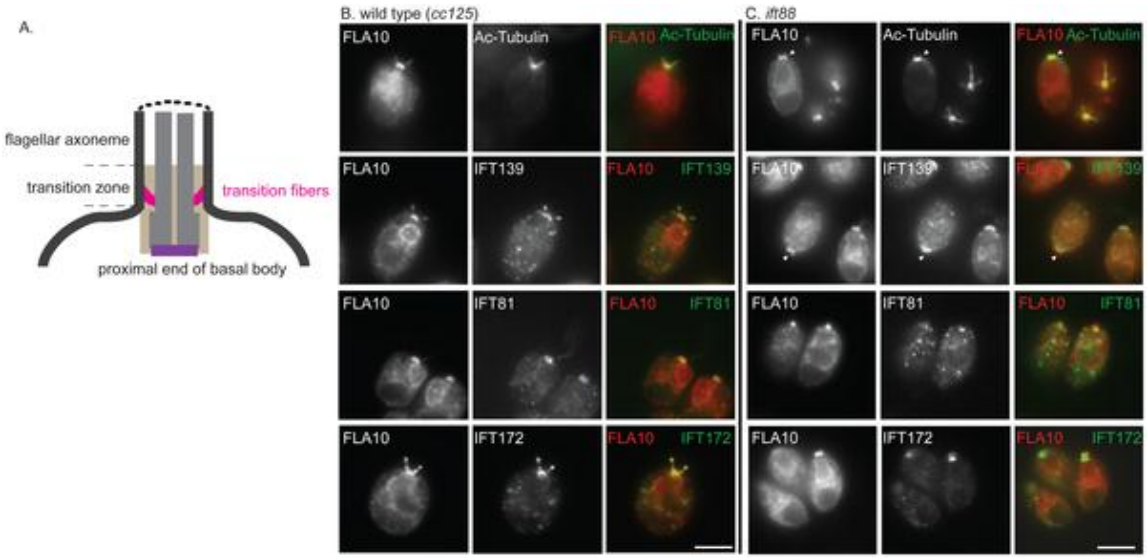

Figure 6. IFT88 is required for localization of complex B proteins to transition fibers of basal bodies. (A) A cartoon to illustrate the position of the transition fibers in the transition zone and the proximal end of a basal body. Immunofluorescent stains showing localization patterns of IFT proteins within the wild type cells (B) and the *ift88* mutant cells (C). The localization of FLA10 showed the cellular sites of transition fibers [36]. Acetylated tubulin (Ac-Tubulin) marked the basal bodies and the flagella emanating from the basal bodies (in wild type). (B) Both A (IFT139) and B (IFT81 and IFT172) proteins colocalized with FLA10 at the basal bodies and extended into the flagella in wild type cells. (B) In *ift88*, IFT139, an IFT A protein, colocalized with FLA10 at the transition fibers. FLA10 was also detected in the very distal part of the transition zone (arrows). Two B proteins, IFT172 and IFT81, however, localized only to the proximal ends of basal bodies. Scale bar, 10 μm.

In wild type cells, IFT complex B proteins, IFT81 and IFT172, which were seen as two straight bands beneath the flagella, colocalized with FLA10 (**Fig. 6B**). However, in *ift88* mutant, both IFT81 and IFT172 no longer colocalized with FLA10, but were instead localized to the proximal ends of the basal bodies, and failed to localize onto the transition fibers (**Fig. 6C**). Thus, although the *ift88* mutant contained the intact complex B core (**Fig. 3C**), the failure to dock the IFT complex B onto transition fibers, the initiation site for flagellar assembly, could explain why the *ift88* mutant cells completely lack flagella [23].

To check if the proximal end basal body localization of complex B proteins requires them to be in the B core complex, the *bld1* mutant, which contains a disrupted

complex B core (**Fig. 3D, E**), was used in immunofluorescent staining analysis (**Fig. 7**). Similar to *ift88* mutant, both IFT81 and IFT172 localized to the proximal ends of the basal bodies, but failed to dock onto the transition fibers (**Fig. 7**). Thus, it is likely that individual complex B proteins are able to localize to the proximal ends of basal bodies, but their subsequent translocation onto the transition fibers require them to be in a completely assembled complex B.

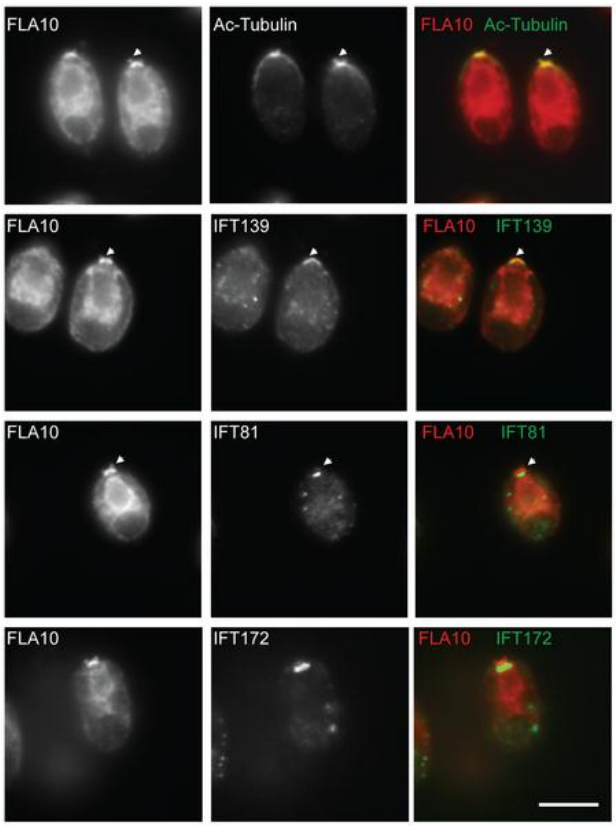

Figure 7. Complex B proteins localize to the proximal end of the basal bodies in *bld1*. Immunofluorescent stains showing localization patterns of IFT proteins within the *bld1* mutant. Acetylated tubulin (Ac-Tubulin) showed the cellular location of basal bodies. FLA10 and IFT139 correctly localized onto the transition fibers of the basal body. FLA10 was also found at the very distal part of the transition zone (arrows). IFT81 and IFT172, two complex B proteins, were found at the proximal end of the basal bodies, but not on the transition fibers. Scale bar, 10 μm.

Discussion

Assembly of IFT Complex B Is Sequential and Basal Body Localization Is a Two-step Process

In this study, we report that three complex B core proteins of *Chlamydomonas* have distinct roles in complex B assembly and stability and apical peri-basal body localization. By analyzing the intermediate complexes formed in mutants *ift46, bld1*, and *ift88* (**Fig. 3**), this report clearly demonstrates that IFT46, IFT52, and IFT88, despite being in the same subcomplex [16], do not contribute equally to the assembly of complex B. The *ift46* mutant cells are capable of assembling a relatively intact complex B, which is likely responsible for the assembly of the short flagella. An intermediate complex, likely containing IFT88/70/52/27/25, was detected in the *ift46* mutant, which may represent a key step in complex B core assembly. Although complex B does assemble in *ift46* mutant, the assembled complex without IFT46 is highly prone to degradation (**Fig. 4D**). The lack of stability could be the leading factor causing low cellular amounts of complex B proteins in *ift46* mutant, which in turn is capable of assembling only stumpy flagella. In contrast, the *bld1* mutant does not contain an assembled complex B core, indicating that IFT52 plays a key role in mediating the assembly of complex B (**Fig. 3D, E**). In *ift88* mutant cells the complex B core still assembles and remains stable (**Figs. 3C** and **4C**). However, the complex B proteins no longer localize at the transition fibers, but instead are restricted to the proximal ends of basal bodies (**Fig. 6C**). The failure of anchoring complex B to the transition fibers is

likely due to the absence of IFT88 itself or one of the peripheral proteins that failed to bind to the complex B. Taken together, these results revealed that the assembly of complex B is through a step-wise process and the localization of complex B involves translocation of complex B from the proximal end to the transition fibers via an IFT88-dependent mechanism (**Fig. 8**). The accumulation of IFT particles on the transition fibers of basal bodies, where flagella assembly initiates, is obviously advantageous to flagellar assembly. This study provides some clues as to how IFT complex B localizes to the basal body. It appears that individual IFT complex B proteins are first transported to the centrioles (**Figs. 6 and 7**), where they assemble into a complex, and then translocate onto transition fibers.

IFT88 Is Critical for Mediating the Attachment of Peripheral Proteins to the Complex B Core

Although IFT88 is a subunit of complex B core, it is not needed for complex B core assembly. Instead, its function is most likely to bind peripheral proteins to the core. Compared to the interactions identified within the complex B core subunits, the interaction between IFT57 and IFT20 is the only one that has been confirmed among the peripheral proteins to date [39]. Interestingly, in *ift88* mutant, the cellular level of IFT57 is greatly reduced compared to other complex B proteins [23]. It is possible that in the absence of IFT88 and IFT57, the rest of the peripheral proteins are no longer able to attach to the complex B core. Future work on the identification of which peripheral protein that interacts with IFT88 and the additional interactions among peripheral proteins should provide a complete picture on the architecture and the assembly of complex B.

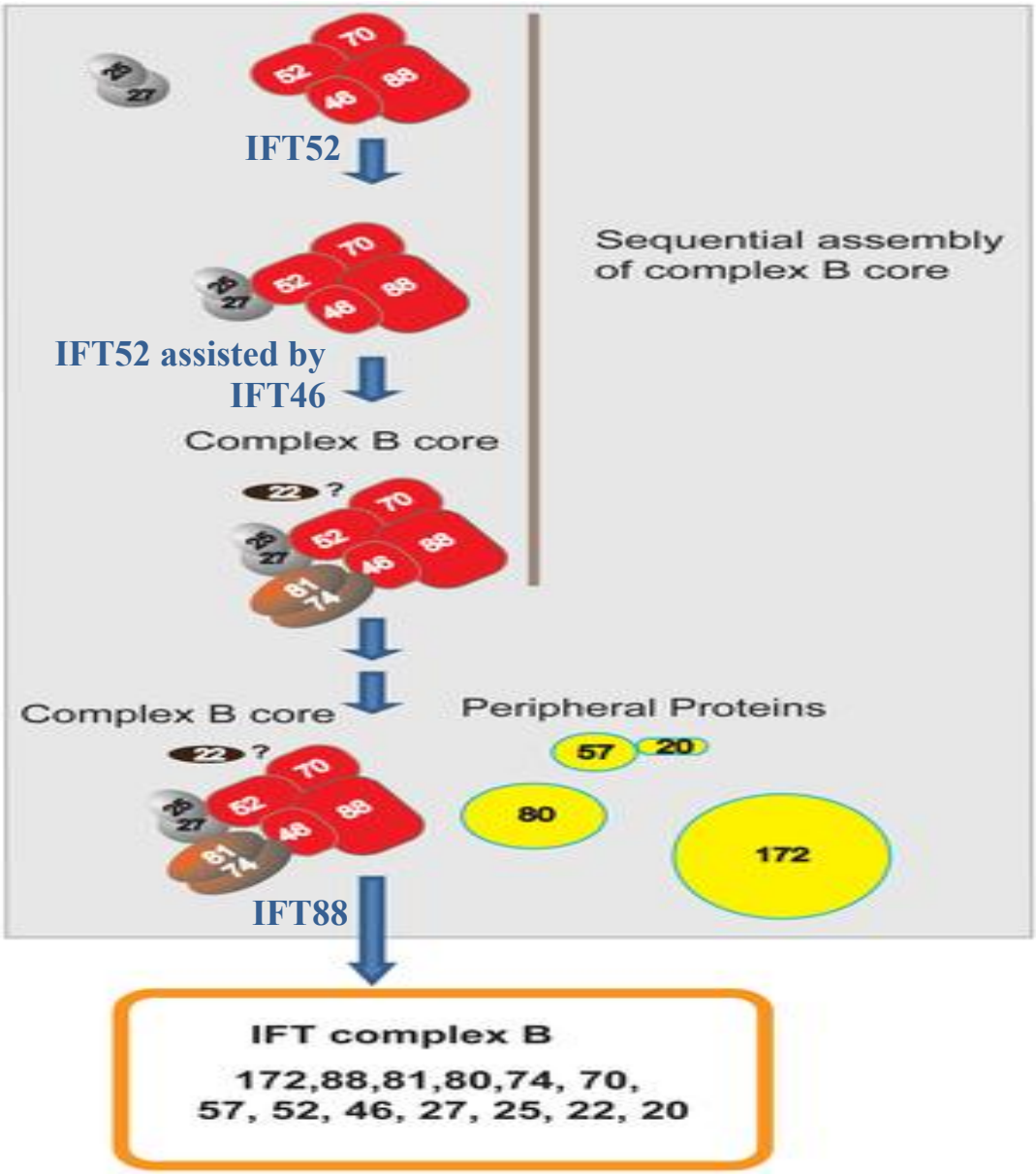

Figure 8. Sequential assembly and basal body localization of complex B. This model shows that during complex B assembly, complex B core assembles and then the peripheral proteins assemble onto complex B core to form an integrated complex B. First, the subcomplexes IFT88/70/52/46 and IFT27/25 binds to form IFT88/70/52/46/27/25, and the binding is dependent on IFT52. The absence of IFT52, as seen in *bld1* mutant, prevents the formation of IFT88/70/52/46/27/25, causing the accumulation of the intermediate transition complexes IFT88/70/46 and IFT27/25. Second, IFT74 and IFT81 assemble onto IFT88/70/52/46/27/25 to form the complex IFT88/70/52/46/27/25/81/74. This step is assisted by IFT46. The absence of IFT46, as seen in *ift46* mutant, either generates unstable IFT88/70/52/27/25/81/74, which is prone to degradation or dissociates the complex into IFT88/70/52/27/25 and IFT81/74. IFT81/74 is insoluble and cannot exist on its own [13]. Thus, although the interaction between IFT74 and IFT81 is strong [12], [13], the complex 81/74 only stably forms while it assembles onto the complex B core. IFT22 is a complex B core protein (data not shown) but currently it is unknown how it assembles into the complex B core. Lastly, the peripheral proteins assemble onto the complex B core to form an intact complex B. IFT88 is not required for complex B core formation, but is essential for mediating the binding of peripheral proteins to the B core. All the assembly steps involved in forming complex B core may occur at the proximal end of the basal bodies. The translocation of complex B from the proximal end of the basal body to the transition fibers is dependent on the presence of IFT88 and proper association of peripheral proteins.

IFT88 and/or Peripheral Proteins Are Essential for Anchoring Complex B on the Transition Fibers

Our results indicate that IFT88 itself, or one of the complex B peripheral proteins that failed to attach to the complex B is responsible for the translocation of complex B from the proximal end of basal bodies onto the transition fibers. This idea can be tested by examining the assembly status and the localization pattern of complex B proteins in mutants of peripheral proteins. However, the set of complex B protein mutants is far from complete, with only a handful of complex B mutants currently available. The IFT complex B proteins are correctly localized to transition fibers in temperature sensitive mutant *fla11/ift172*^{ts} (data not shown). Thus, it is unlikely that IFT172 is responsible for complex B transition fiber localization, although this result needs to be confirmed once a null mutant of *ift172* is available. Recently, an *ift80* mutant (likely a null mutant) was identified; like *bld1* and *ift88* mutants, this mutant is completely flagella-less with no axonemal microtubules assembled [40]. Further studies on the assembly status and the localization pattern of complex B proteins of the *ift80* mutant should provide answers to the function of IFT80 in complex B assembly and localization.

The Anterograde Motor Fla10-kinesin-II Must Be Recycled Back to the Cell Body After Each Trip to the Flagellar Tip

IFT particles undergo constant bi-directional transport along the entire length of flagella to support flagellar assembly and maintenance. This report shows that both IFT particle proteins and the anterograde motor Fla10-kinesin-II have very low turnover rate (**Figs. 4** and **5**). By analyzing the motility of GFP tagged proteins, previous studies have

observed an interesting discrepancy of the movement between the IFT particle proteins and the Fla10-kinesin-II. IFT particle proteins display both the anterograde and retrograde transport. In contrast, Fla10-kinesin-II only shows the anterograde transport. No retrograde transport can be observed for Fla10-kinesin-II [41,42], leading to the possibility that Fla10-kinesin-II is discarded at the flagellar tip after completing one anterograde transport and never recycled back for reuse. However, here we show that Fla10-kinesin-II is very stable (**Fig. 5**). No protein amount change of FLA10 can be detected after 16 hours of treatment with cycloheximide. Thus, normally there must be little, if any, new Fla10-kinesin-II synthesized in the cell body. The protein synthesis for Fla10-kinesin-II can be up-regulated when the protein turnover rate is increased, as seen in both *fla10*^{ts} and *fla3-1b* mutants. Such upregulation is likely required to replenish the depleted Fla10-kinesin-II protein due to increased degradation rate. Because the turnover rate of Fla10-kinesin-II is extremely low, it has to be reused to power numerous rounds of IFT movement. Therefore, Fla10-kinesin-II must be efficiently recycled back to the cell body after each trip to the flagellar tip.

Materials and Methods

Strains and Culture Conditions

Strains used as controls included *Chlamydomonas reinhardtii* wild type strain *cc125* and cell wall deficient, but otherwise wild type strain *cw92* (CC-503). The *cw92* strain was used for the sucrose density gradients, as the cell wall deficiency made it easier to lyse the cells for protein extraction. These control strains along with mutant strains, *ift88* (CC-3943) [23], *ift46* [27], *bld1* (CC-477) [26], *fla10* null (CC-4180), and

temperature-sensitive mutants *fla10*^{ts} (*fla10-1* allele, CC-1919*)* and *fla3-1* (CC-4283) were obtained from the *Chlamydomonas* Center (http://www.chlamy.org). The strains were cultured on Tris-acetate-phosphate (TAP) solid plates or TAP liquid media with constant aeration in a Conviron programmed at 22°C in continuous light.

Whole Cell Protein Extracts and SDS Page Electrophoresis

20 mL TAP liquid media was inoculated with a loop of cells from a fresh (within a week old) TAP solid plate culture. Liquid cultures were grown for approximately 3 days (until medium to dark green) under the above conditions. The cultures were normalized based on the lightest colored culture by adding TAP liquid media to the others until all cultures were about the same color. 1 mL of culture was spun down at 14000 RPM for 5 minutes and the supernatant was removed. The cell pellet was then resuspended in 50 µL 1X PBS. 50 µL 2X laemmli buffer was then added and the cultures were vortexed for 30 seconds. The samples were then boiled for 3 minutes, and spun down for 10 minutes at 14000 RPM. The supernatant was collected and stored at -20ºC for short- term or -80ºC for long-term storage. Samples were used for direct electrophoresis using SDS Page gels. 5 µL of sample was added to each well, then protein amounts were adjusted based on total lane intensity detected on gels stained with Coomassie Blue using ImageLab^{TM} Software (BioRad).

Cycloheximide Treatment

Cells were cultured under the conditions described above. Protein was extracted using above protocol prior to treatment to be used as control samples. The remaining culture was treated with 10 µg/ml cycloheximide and again placed in the conviron under

the same culture conditions as pre-treatment. Protein was then extracted at multiple time points using the same methods used when extracting control samples.

Western Blotting

Protein was separated on a 10% SDS Page gel, then electro-transferred to a polyvinylidene difluoride membrane. Proper transfer was tested using ponceau staining. Membranes were then blocked in 5% nonfat dry milk in TBST (10 mM Tris, pH 7.5, 166 mM NaCl, plus 0.05%Tween-20) with .02% sodium azide. Membranes were then incubated in primary antibody in blocking solution for at least 1 hour (up to one day for weaker antibodies). They were then washed 4 times for 10 minutes each time in TBST. Membranes were then incubated in secondary antibody in 5% nonfat dry milk in TBST for at least one hour, followed by an additional 4 washes using TBST. Chemiluminescence with X-ray film was used to detect antibody bands.

Antibodies

Antibodies used in this study included antibodies against α-tubulin (clone B-5-1-2, ascites fluid; Sigma); IC69 (clone 1869A; Sigma); acetylated tubulin (clone 6-11B-1, ascites fluid; sigma); and IFT polypeptide antibodies included antibodies to *Chlamydomonas reinhardtii* IFT172, IFT81, IFT139 [9], IFT122 [11], IFT74 [43], IFT46 [27], IFT25 [14], IFT27 [34], and FLA10 [9].

Sucrose Density Gradient

500 mL of cells were grown under conditions described above. Cells were then pelleted and resuspended in autolysin and shaken under light for 1 hour or until cells separated and were able to be lysed by 1% Triton. Cells were again pelleted and stored at

-80ºC. After thawing on ice, cells were resuspended in 10X HMDEK with DTT, followed by serial centrifugation of the supernatant at 4º C until supernatant was a clear yellow/green. High and low density sucrose solutions that contained 1X HMDEK were prepared in 12 mL centrifuge tubes and were made into gradients. The supernatant was placed on top of the sucrose gradients, then centrifuged at 37000 RPM at 5ºC for 18 hours. A No Drop Counter apparatus was used to collect 500-550 µL fractions. Enough 10X Laemmli buffer was added to each tube to make the sample 1X laemmli buffer. Samples were stored at -20ºC (or -80ºC for long-term storage).

Approximate S-values were derived using the sedimentation behavior of the following proteins with established S-values: the prominent ~55 kDa large subunit of RuBisCo sedimenting at ~19S, FLA10 with known sedimentation at about 10S [9], and cytoplasmic radial spoke complex at 12S [43].

Immunofluorescent Staining

Cells were fixed in methanol and blocked with blocking buffer (5% BSA, 1% Cold Water Fish Gelatin, 10% goat serum in 1X PBS). Cells were then incubated in primary for 4 hours at room temperature or overnight at 4ºC followed by washing in 0.5X PBS. Cells were incubated in secondary antibody for 1 hour at room temperature. SlowFade Antifade Reagent (Invitrogen) was used to prevent loss of signal. Cells were viewed under an Olympus IX-70 inverted fluorescence microscope at 100X magnification. An Image Point CCD Camera (Photometrics) was used to capture the image through PCI Software.

CHAPTER III

IDENTIFYING INTERACTIONS BETWEEN CORE AND PERIPHERAL PROTEINS

Introduction

The aforementioned results give us a better understanding of the interactions among core proteins during assembly and localization. However, little is revealed about the interactions between core and peripheral proteins. Discovering how peripheral proteins assemble onto the core could lead to a better understanding of the functions of these proteins for ciliogenesis. The differing phenotypes of *ift46*, *bld1*, and *ift88* mutants can now be explained. *Ift46* is able to produce short flagella because it still assembles a nearly complete but unstable functional complex B. *Bld1* has a highly disrupted complex B core, which causes complex B to be dysfunctional, leading to a flagella-less phenotype. Although *ift88* still forms a somewhat complete complex B, it seems to still be missing some components necessary to localize complex B to the transition zone, making the mutant unable to perform ciliogenesis. It is unlikely that IFT88 is responsible on its own for proper localization. Conversely, we predict that IFT88 interacts with at least one peripheral protein that is important for the localization of complex B to the initiation site for ciliogenesis. Here we use yeast two-hybrid assays [29] to determine protein interactions between IFT88 and peripheral proteins. So far, the only interaction known between the peripheral proteins is IFT57 and IFT20 [39]. Therefore we will also

identify the interactions between peripheral proteins themselves to further investigate peripheral assembly and architecture.

Results and Discussion

This project is currently in progress, so there is little to report at this time. Yeast two-hybrid assays [29] will determine the interactions between IFT88 with peripheral proteins IFT20, IFT57, IFT80, and IFT54. In addition, binding ability between IFT20 and IFT80, IFT20 and IFT54, IFT57 and IFT80, IFT57 and IFT54, and IFT80 and IFT54 will be tested to determine the peripheral architecture of complex B.

Primers were designed for each gene so that when the fragments were amplified, they would contain restriction enzyme sites at both ends. These fragments were then ligated into TA cloning vectors and transformed into *E. coli*. The plasmids were extracted and purified from the transformants. Next, they were digested with the respective restriction enzymes and tested by gel electrophoresis for the presence of the gene and for its ability to digest completely. When confirmed, the digested fragments were then ligated into plasmids that allow the expression of fused proteins containing either a GAL4 activation domain or binding domain. This is the current stage of the project. When the ligations are confirmed, they will be transformed into yeast. The reporter gene, LacZ, will only be transcribed if both the activation and the binding domains are able to bind onto the DNA to recruit polymerase. If the bait protein (fused to GAL4 binding domain) directly interacts and binds to the prey protein (fused to GAL4 activation domain), transcription of LacZ will be activated in the presence of IPTG to allow the production of β-galactosidase. This will break down supplemented X-

Gal to produce colonies with a blue color, allowing selection of protein combinations with positive binding ability [29]. This system will allow us to determine which of these peripheral proteins bind to each other and which can bind to the IFT88 core protein. This knowledge is important to add to the current understanding of the architecture of IFT complex B because it will lead to a better grasp on how complex B works as a whole to allow the proper performance of IFT and ciliogenesis. The more we understand about this process, the more likely our research will lead to practical applications in preventing ciliopathies.

Materials and Methods

Strains and Culture Conditions

TOP10 (Invitrogen™) chemically competent *E. coli* strains were used for TA cloning of the PCR products. JM109 cells were used for transformation of the pGADT7 and pGBKT7 ligations into *E. coli* to confirm the insertion and to isolate and purify the plasmids for transformation into yeast. *E. coli* strains were grown in solid or liquid LB media with either Ampicillin or Kanamycin for selection, depending on the plasmid antibiotic marker. IPTG and XGal were also supplemented on the plates when necessary for blue/white colony screening. For transformations, plates were incubated at 37ºC overnight. Selected colonies were grown at 37ºC in liquid LB with antibiotic overnight to be used for plasmid purification.

The yeast strain used was AH109 (Clontech). This strain helps prevent false positives since it contains *ADE2, HIS3, lacZ* and *MEL1*, which are reporter genes that have promoters which respond to GAL4. Transformants were grown on SD/-Ade/-His/-

Leu/-Trp/X-gal to ensure that the only blue colonies were true positives with the bait and prey fused proteins bound to each other, allowing the transcription of LacZ and the production of β-galactosidase. Cultures were grown in accordance with the Matchmaker™ GAL4 Two-Hybrid System 3& Libraries User Manual (Clontech).

Plasmids

TOPO TA vectors (Invitrogen™) were used for cloning gene products to allow for more efficient digestion in order to generate effective ligations into vectors used for yeast transformation. These vectors were pGADT7, which produces a protein product fused to GAL4 DNA activation domain (prey), and pGBKT7, which produces a protein product fused to GAL4 DNA binding domain (bait). Both of these vectors contain a T7 promoter which allows for the expression of the fused proteins. They also include two origins, pUC for replication in *E. coli* and 2 μ for replication in yeast. pGADT7 contains an Amp^r marker and a *LEU2* nutritional marker for selection in *E. coli* and yeast, respectively. pGBKT7 contains an Kan^r marker and a *TRP1* nutritional marker for selection in *E. coli* and yeast, respectively.

Primer Design

Primers were designed so that the entire gene from each of the selected proteins could be amplified from a cDNA clone template. In addition, restriction enzyme sequences were added to the 5' ends of the primers to allow for future ligation into the plasmids that will be transformed into yeast (**Table 1**). Enzyme sequences were selected so that when ligated into the yeast plasmids, they would not change the reading frame. Enzyme sequences that were present within any of the genes were generally avoided so

that we did not have the risk of inserting an incomplete gene into the plasmid. For all genes except *IFT80*, the selected enzymes were *NdeI* for the forward primers and *EcoRI* for the reverse primers. *IFT80* was an exception since it contained an *EcoRI* site within the gene. In this case, *BamHI* was used for the reverse primer instead of *EcoRI*. An extra GC was added to the 5' end of each primer to prevent the degradation of the enzyme sites at the ends of the PCR products.

Table 1. Primers Used for Yeast Two-Hybrid Assay

Gene	Primer Sequence	Restriction Site
IFT88 (Forward)	GCCATATGAGCTACGGGGGCACGGAG	*NdeI*
IFT88 (Reverse)	GCGAATTCTTACATGGGCAGCAGGTCGTCC	*EcoRI*
IFT80 (Forward)	GCCATATGCGTCTCAAGGTCAAGCAGTCCAG	*NdeI*
IFT80(Reverse)	GCGGATCC TTACACGTAGCGCTTGGCG	*BamHI*
IFT57 (Forward)	GCCATATGCCGCAGGAAATGCTGGCCG	*NdeI*
IFT57 (Reverse)	GCGAATTCCTAGTCCTCCTCCTCGTCACTG	*EcoRI*
IFT54 (Forward)	GCCATATGTGCGATAACTGGCAGGCAACCATTG	*NdeI*
IFT54 (Reverse)	GCGAATTCTTACCGCCCAGCGGTTGCC	*EcoRI*
IFT20 (Forward)	GCCATATGGACGCGGTAGATAGAGGAGTCTACT	*NdeI*
IFT20 (Reverse)	GCGAATTCTTACACGTATGCCGCCCCGC	*EcoRI*

PCR

PCR was used with the above primers to amplify genes from clones, cDNA, or a cDNA library. These amplified fragments were inserted in TA cloning vectors for efficient digestion. For PCR reaction and program information see Secondary RESDA methods in the next chapter.

Cloning and Plasmid Extraction

PCR products were cloned into TOPO TA vectors and transformed into chemically competent TOP10 *E. coli* strains using the TOPO® TA Cloning® Kit for

subcloning with TOP10 *E. coli* (Invitrogen™)**.** pGADT7 and pGBKT7 ligations containing the desired gene inserts were transformed into JM109 Chemically competent cells using the transformation protocol found in the pGEM®-T and pGEM®-T Easy Vector Systems Quick Protocol (Promega). Plasmids were extracted using the GeneJET™ Plasmid Miniprep Kit (Fermentas). Protocols found in the Matchmaker™ GAL4 Two-Hybrid System 3 & Libraries User Manual (Clontech) were used for transformations intoAH109 yeast cells.

Digestions and Ligations

TA plasmids were double digested with the inserts' respective restriction enzymes (Fermentas). Gel electrophoresis was used for double digests to separate the fragments from the plasmids. This allowed confirmation that the TA cloning was successful. Fragments were purified with the GeneJET™ Gel Extraction Kit (Fermentas). These purified fragments were ligated into pGADT7 and pGBKT7using T4 DNA Ligase (Invitrogen).

CHAPTER IV

IDENTIFICATION AND CHARACTERIZATION OF RANDOM INSERTIONAL FLAGELLAR MUTANTS

Introduction

Little is known about the functions of the peripheral B proteins, how they are assembled onto complex B, and what their functions are in localizing, regulating, and stabilizing the complex. So far, there are only a couple mutants available for peripheral B proteins, among these are *fla11* [31] (temperature sensitive mutant for IFT172) and *ift80* [40] (likely a null mutant). Though these mutants will be useful for gaining insights into the functions of these proteins, it is important to screen for new mutants of the other peripheral proteins in order to develop a complete picture of the inner workings of complex B for ciliogenesis.

To attempt to identify a novel IFT complex B peripheral mutant in *Chlamydomonas reinhardtii*, random insertional mutagenesis was performed. Mutants were then screened for flagellar defects and flanking sequences were identified using restriction enzyme site-directed amplification (RESDA) PCR [30]. A few interesting mutants have been identified, but none thus far that are of interest to this project. RESDA screening will continue in hopes of identifying a peripheral protein novel mutant, which would be a great tool to determine the roles that the periphery of complex B plays on the stability, assembly, and localization of IFT complex B.

Results and Discussion

Random Insertional Mutagenesis

Novel *Chlamydomonas* IFT and flagella-related mutants were created by randomly inserting a linearized plasmid into the genome of wild type cells. The plasmid used contains a hygromycin resistant gene allowing for selection in media supplemented with the antibiotic. Restriction enzyme *ScaI* was used to linearize the plasmid during the production of the first few sets of mutants. The plasmid only has one *ScaI* site available for digestion, so the inserted fragment was the entire 4.4 kb plasmid. It proved to be very difficult to work with these mutants due to possible religation or failure to digest the plasmid properly, multiple inserts throughout the genome, or a chain of inserts within a gene (**Fig. 9**). It is unclear whether our difficulty was due to the size or nature of

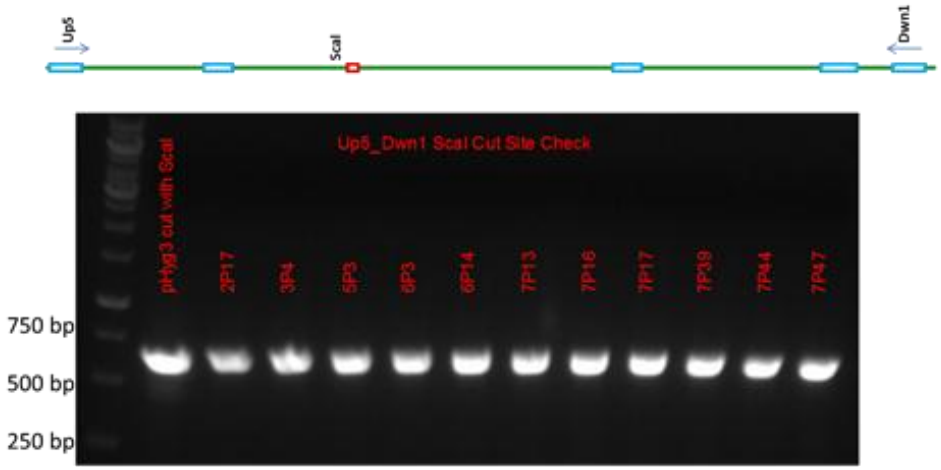

Figure 9. Multiple insertions or improper digestion of plasmids are common among random insertional mutants made with pHyg3 cut with *ScaI*. Eleven mutants and the digested fragment of pHyg3 were tested using primers Up5 and Dwn1, which are found on either side of the *ScaI* restriction site. All templates produced fragments at the predicted size of ~630 bp. These results show that the plasmid either failed to digest at *ScaI*, somehow religated itself, or there are multiple consecutive inserts in each of the tested mutansts.

the insert, but we changed the procedure for the new sets of mutants to see if reducing the size of the inserted fragment would make the screening and identification process more efficient. For the newer mutants, the enzyme *HindIII*, having two restriction sites, was used to cut out the fragment containing just the promoter, hygromycin resistant gene, and untranslated region of pHyg3 so that it still could express the marker gene. Mutants made with these much smaller 1.7 kb fragments showed to be more consistent, with fewer multiple inserts or strange ligation and digestion behavior, making identification of the disrupted gene much more feasible. However, many of these strains are most likely not null mutants for any particular gene and would be difficult to characterize since they had insertions in extragenic regions. To attempt to solve this problem, future mutants will be made using a PCR product that contains the hygromycin gene but lacks the promoter. This means that the only time a transformant will be able to survive on hygromycin would be when the fragment was successfully inserted inside a gene, using the genomic promoter to express the selective marker gene. This technique should greatly increase the chances of getting a null mutant from the screening process.

Screening for IFT Mutants

For this project, our main interest is in peripheral IFT B genes that do not yet have null mutants available to the research community, such as *IFT57*, *IFT20*, or *IFT54*. To screen for potential flagellar mutants, strains were first tested for a failure to phototax (**Fig. 10**). Cells that were unable to swim toward light most likely had a sensory dysfunction and/or deformed and malfunctioning flagella. All strains that could perform phototaxis were discarded and all phototaxis negative strains were then examined under

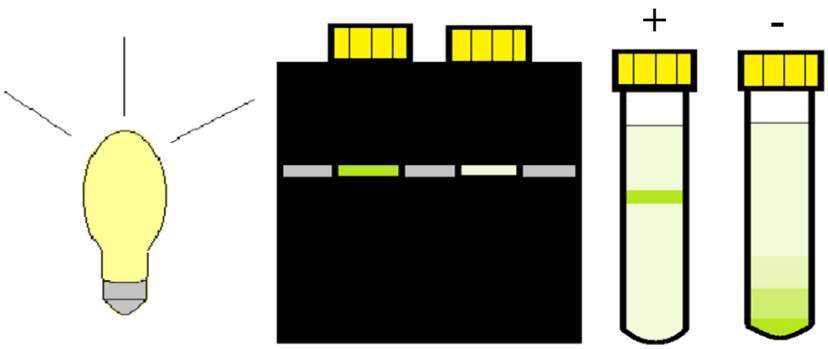

Figure 10. Phototaxis assay. Cultures in liquid TAP media were placed in test tubes and incubated in a phototaxis box in which only one slit of light could shine through. Phototaxis strains showed a distinct line of green where the light shone through, while phototaxis negative mutants had a homogenously green culture solution or had cells sink to the bottom of the tubes.

the microscope. Each strain was characterized and categorized based on its visible flagellar phenotype. Because some mutants had multiple or inconsistent phenotypes, it is advisable to grow several single colonies from each mutant to eliminate contamination and separate mixed strains for accurate analysis before attempting to identify the mutated gene. A variety of phenotypes were observed including mutants with flagella that were short, long, have unequal length, abnormal number, motility deficiency, or atypical accumulation of proteins. For this study, strains with short or no flagella (bald) were of the most importance, since these are typical phenotypes seen in known IFT B mutants. However, the proteins most interested in are not core proteins, so they may have less of an effect on ciliogenesis but may be involved in a more discreet function. Therefore, mutants with phenotypes besides bald or short flagella were not ruled out.

In addition to the phototaxis assay and microscopic analysis, western blotting was also useful for narrowing down the mutants to ones likely to be null for complex B proteins. Typically a strain that is deficient in a complex B protein will show the pattern of a reduction in other B proteins and an increase or lack of change in IFT A proteins,

while maintaining a normal expression of IFT motor proteins. Conversely, an IFT A mutant typically has a reduction in other IFT A proteins, while B protein expression remains the same or is increased. Twenty-two bald mutants were tested for patterns characteristic of an IFT B protein mutant by probing with one A, one B, and one motor protein antibodies. Based on their expression patterns, three mutants were identified as potential IFT B mutants while two showed similar patterns to complex A mutants. In addition, one mutant showed normal expression of both IFT A and B proteins, but had a drop in FLA10 motor protein production, making this a possible IFT motor mutant (**Fig. 11**).

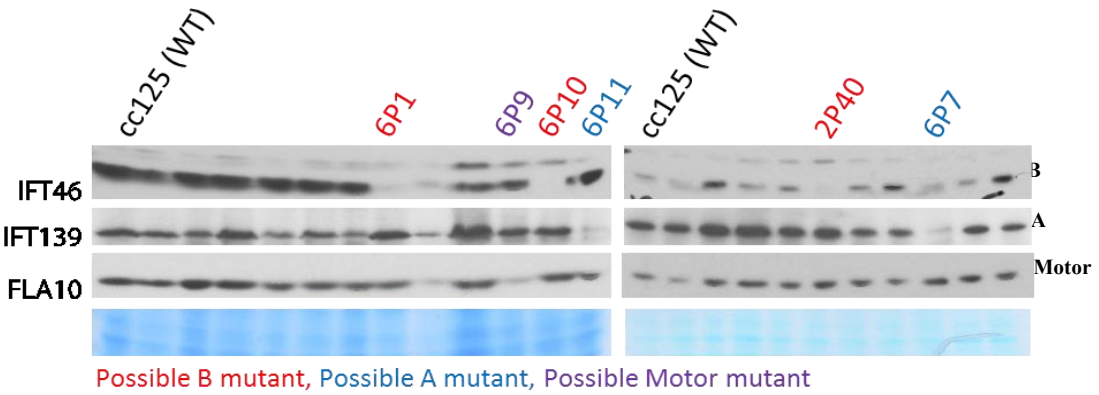

Figure 11. Western blot analysis of whole cell extracts revealed potential IFT mutansts. 6P1, 6P10, and 2P40 are possible B mutants, having a reduction of IFT B protein expression, while maintaining or increasing the expression of IFT A proteins. 6P11 and 6P7 are potential A mutants, having a reduction in expression of IFT A proteins, while maintaining expression of IFT B proteins. 6P9 may be a motor protein, since it has a reduction in a motor protein, but not in IFT A or B protein expressions. Coomassie staining shows the relative loaded protein amounts.

To test the mutants for mutations in specific IFT genes, primers were designed to amplify the genes of interest using PCR. If the insert disrupted the gene, the primers would not yield a result since there would be either a shift in the genomic sequence or a deletion, preventing efficient amplification of the fragment. Many mutants were

screened using this method, but all mutants tested produced a band for each set of primers, thus yielding no confirmed mutations in the desired genes. This method of screening, although it can be specific to a particular gene and performed quickly in high quantities, proved to be an inefficient way to identify mutated genes in the case of our mutants. Therefore, restriction enzyme site-directed amplification (RESDA) PCR [30] was applied as a sequencing approach to the identification of the mutations.

RESDA PCR

RESDA PCR is a way in which one can amplify flanking sequences of an inserted fragment so that they can be sequenced for identification of a disrupted gene. Two PCR reactions were performed for this method. Degenerate primers, which included a restriction enzyme sequence and a known sequence (Q0), were paired with primers homologous to known insert sequence near the ends of the fragments for the primary RESDA reaction (**Fig.12**). Degenerate primers, on their own, are mostly nonspecific and can bind to almost anything. The restriction enzyme sequence within

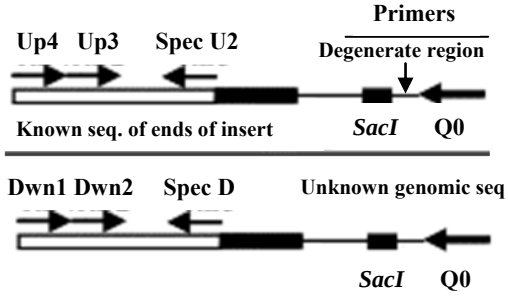

Figure 12. RESDA PCR. Degenerate primers contain a restriction enzyme sequence which allows binding at restriction sites throughout the genome. When one binds close enough to the insert, a product containing the flanking sequence of the insert can be made. The primary RESDA PCR is performed by amplifying the insert flanking sequence using Up4 and degenerate primers for one end of the insert, and Dwn1 and degenerate primers for the other end. The primary product is then used as the template for the secondary reaction which amplifies the fragment with Up3 and Q0 primers for one end, and Dwn2 and Q0 for the other. SpecU2 and SpecD are used to test the specificity of the Up and Dwn primers, respectively.

these primers allowed them to selectively bind to any site in the genome that contained its respective restriction enzyme sequence. When the primers were bound to a region that was near the insert, a product was formed with the primers on the ends of the insert. A secondary reaction was used to increase specificity of the product. For this reaction, the product from the primary reaction was reamplified using a primer that matched the known sequence (Q0) on the degenerate primer and one closer to the end of the inserted fragment than the previously used insert primer (**Fig. 12**). The reason we did not use the same insert primer was to increase the efficiency of the PCR since amplifying the very end of a sequence often does not yield clean results. The product of the secondary PCR reaction was then run on a gel and bands that were large enough to include enough genomic sequence were extracted for sequencing [30].

The success of this procedure relied not only on the methods used for mutagenesis but also on how the PCR was performed. Standard Taq polymerase and buffer were used in the first RESDA attempt, yielding smeared bands and bands that were too small to include enough genomic DNA for sequencing. To resolve this problem we started using GoTaq® DNA Polymerase and buffer (Promega), which are more robust and reliable reagents for amplification of products that are problematic, such as ones amplified with degenerate primers. Although these reagents greatly increased the success rate, the high efficiency of amplification of even the smallest amount of DNA template made the PCR much more prone to the effects of contamination. Much time was spent on troubleshooting contamination issues, and it is advised to take all necessary precautions to prevent these issues during handling of reagents and DNA. Contamination

issues aside, RESDA PCR has shown promise in identifying flagellar mutants from our screen in an efficient and effective way.

Identification of *IFT80*, *PF16*, and *CEP290* Mutants

Thus far, five flagella-related mutants have been identified using the RESDA PCR method. Among these are *IFT80* (**Fig. 13 A**), *PF16*, and *CEP290* mutants. Since null mutants for these genes are already available to the scientific community, these mutants did not strike our immediate interest and we are continuing to screen for more interesting novel mutants. However, the three strains may still prove useful in the future for projects relating to these proteins.

IFT80 is an IFT B peripheral protein that has been linked to serious ciliopathies such as Jeune asphyxiating thoracic dystrophy[44] and short-rib polydactyly syndromes [45]. It also has been shown to play roles in important pathways such as the hedgehog signaling pathway [45]. Here, the mutant that had a disruption in *IFT80* had short flagella that were immotile. This is unlike the bald phenotype of the previously discovered *Chlamydomonas ift80* [40] mutant, meaning it could be that our mutant is not null for *IFT80* or that it is not an *IFT80* mutant at all. Since our strain is able to produce flagella, the cells either have some functioning IFT80 proteins available for IFT, or the phenotype of the previously identified *ift80* mutant [40] was not characterized properly. The region of our sequencing result that matched nearly perfectly with IFT80 was about 200 bp, so there is little chance it was a false match. PCR was used to attempt to confirm the mutation (**Fig. 13B, C**). First a primer from the matched region of IFT80 was used with a primer from the end of the insert so that if the sequencing results were correct, the

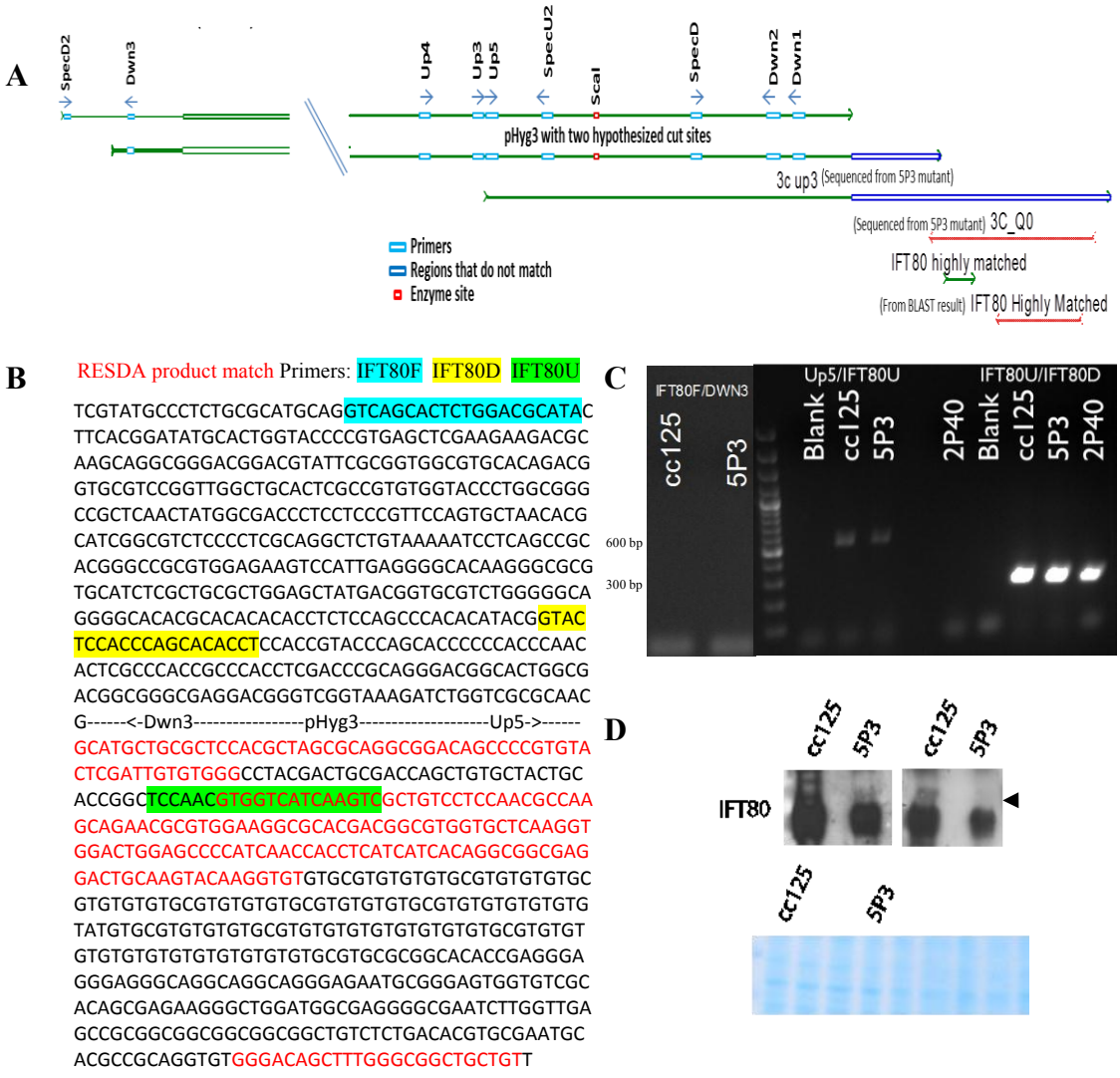

Figure 13. A possible *IFT80* mutant is yet to be confirmed. (**A**) Sequencing results of mutant 5P3 using both Up5 and Q0 primers showed that the flanking sequence matched a ~200 bp portion *IFT80*. Results also showed that the plasmid was either not cut at *ScaI* as expected or that there were multiple consecutive inserts. Two inserts are shown with hypothesized cut sites. The first is based on when our fragment's sequence stopped matching pHyg3 and the second is based on when it started matching *IFT80*. (**B**) *IFT80* sequence with predicted location of the pHyg3 insert. Primers used for confirmation are highlighted. (**C**) PCR and gel electrophoresis showed that wild type and 5P3 did not produce a band with IFT80 and Dwn3 primers. Nonspecific bands were amplified with Up5 and IFT80U primers. Amplification with IFT80U and IFT80D showed that wild type and 5P3, along with another mutant 2P40, all have intact *IFT80* sequence in the region that was expected to be disrupted. (**D**) Western blot analysis showed a possible band for IFT80 in 5P3, but the antibody is too dirty and nonspecific to trust.

DNA from the mutant would produce a product. However, the results were inconclusive since wild type and mutant DNA both produced a nonspecific band. A primer from the other end of the insert along with a primer within the presumed flanking *IFT80* sequence

produced no bands in either wildtype or the mutant. This is also inconclusive, but it could mean that the insertion caused a deletion in *IFT80* so that the flanking sequence is not as predicted. Two *IFT80* primers that were on either side of the expected insert location were also used. Results showed that the mutant still had an intact *IFT80* fragment where we previously thought it was disrupted. It is possible that there was contamination of the strain with wild type or one of the other mutants to produce this band. In addition, when probed with IFT80 antibodies, western blots showed that IFT80 was present in the mutant (**Fig. 13 D**). However, this result cannot be trusted since the antibody is dirty and may be nonspecific. A new antibody should be made to confirm this result. Apart from the initial sequencing analysis, all the results cause doubt in this mutant and more work needs to be done to determine if it is in fact an IFT80 mutant. Since this gene already has a mutant available, it was set aside for future analysis.

A *PF16* mutant was also produced from the RESDA PCR screen. PF16 is a central pair protein that is involved in flagellar motility most likely by maintaining the stability of the C1 central microtubule [46]. Both our mutant and *Chlamydomonas pf16* [46] share a common paralyzed phenotype, which is consistent with a central pair deficient axoneme. To further support that this is a *PF16* mutant, PCR with two *PF16* primers flanking the location of the insert (**Fig. 14A**) were used to test for disruption in the gene. As expected, wild type produced a very strong band at the predicted size of ~300bp, while the mutant only produced an indistinguishable smear. In addition, a *PF16* primer and a primer near the end of the insert (**Fig. 14A**) were able to amplify a ~1200 bp band in the mutant, but not in wild type (**Fig. 14B**). These PCR results and the

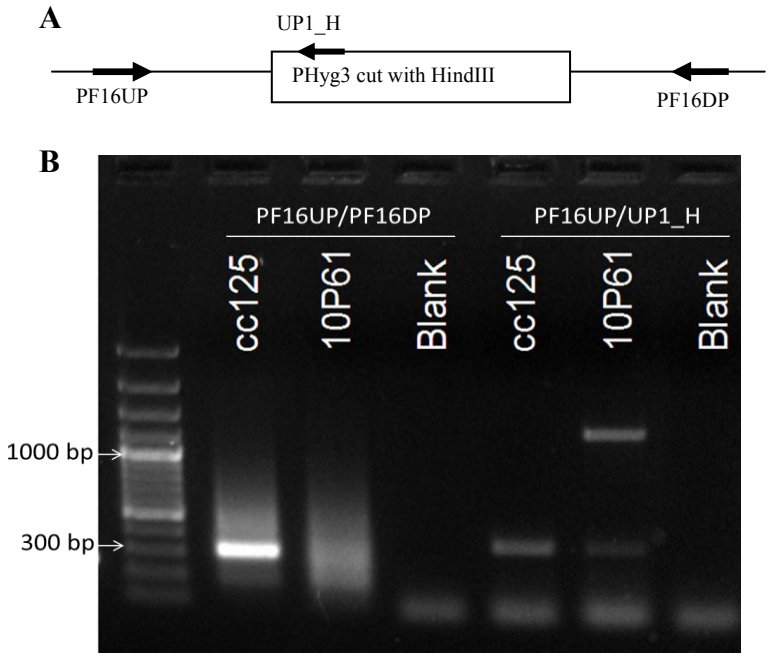

Figure 14. 10P61 may be a *PF16* mutant. (**A**) A diagram shows the relative positioning of the primers used for mutant confirmation. (**B**) 10P61 does not have an intact *PF16* fragment between PF16UP and PF16DP. 10P61 produces ~1200 bp fragment when amplifying with PF16UP and UP1_H. This data supports that 10P61 is a *PF16* mutant.

phenotype consistent with a central pair mutation make us more confident that we have a *PF16* mutant. Further PCR and sequencing, back-crossing, and rescue of the phenotype will confirm the mutation. Again, since there is already a *PF16* mutant available, this mutant was not pursued.

Lastly, a mutant was identified to have a disruption in *CEP290*, a gene that codes for a microtubule protein in the transition zone that is required to link the flagellar membrane to the microtubules and to regulate flagellar protein trafficking [47]. The bald phenotype of our mutant, however, does not coincide with the short flagella phenotype of the known *cep290* mutant. It is necessary to review the phenotype of our mutant to determine if it has a confirmed mutation in *CEP290*. *CEP290* is highly studied and

already has a mutant available, so there was no desire to proceed with confirming this mutant.

Future Aspirations

Now that we have established the methods necessary to efficiently identify mutants from the random insertional mutant screen, we can now build a library of interesting flagellar mutants. The goal is to identify as many mutants as possible, so that there will be many to choose from when forming a solid project. The most useful mutants for this project would be mutations in complex B proteins, preferably from the periphery, to add to the structural assembly and localization work that was done with the core proteins. Once these mutants are identified, they will first be backcrossed and confirmed using PCR, western blotting, and rescuing the phenotypes. The confirmed mutants will then be characterized similar to the characterization that was done for the core protein mutants, *ift46*, *bld1*, and *ift88*. First, an in-depth phenotypic analysis will be performed to determine the protein's function in maintaining proper flagellar morphology. Sucrose density gradients will show if these peripheral proteins impact the assembly of the complex. Cycloheximide time-course treatments will reveal how these proteins affect the stabilities of other IFT and motor proteins. Lastly, immunofluorescent staining will indicate whether or not the protein is necessary for the correct localization of IFT to the transition zone to allow for initiation of ciliogenesis. Results from these assays will further expose the function of the complex B periphery and will be a great addition to the core complex protein study to create a more complete picture of how complex B works as a whole during the IFT process.

Materials and Methods

Strains and Culture Conditions

Mutated strains were created using the wild type *cc125* strain from the *Chlamydomonas* Center (http://www.chlamy.org). Cells were grown in a Conviron with continuous light and aeration at 22ºC. Strains were grown on solid Tris-acetate-phosphate (TAP) plates supplemented with hygromycin when necessary for selection or liquid TAP media.

Mutagenesis

Wild type cells were grown until density reached ~$2x10^6$ to $2x10^7$ cells/ml (dark green). Cells were collected by gently spinning and were resuspended in autolysin and shaken until cells were able to completely lyse in 1% Triton. Cells were again harvested by gentle centrifugation and then resuspended in TAP media. Next, about 4 µg of DNA (linearized and purified) was transformed into the cells using the glass bead method. Cells were allowed to recover in the dark for 24 hours and were then collected with gentle centrifugation and resuspended in a small amount of TAP. They were transferred to a TAP plate with hygromycin for selection. Plates were exposed to light for 6-8 days and about 100 colonies formed for an efficient transformation. Each colony was picked and cultured for screening.

For the first sets of mutants, pHyg3 [48] plasmid DNA linearized with *ScaI* was transformed into the cells. More recent mutants were created by transforming a much smaller fragment containing the hygromycin resistance gene by digesting pHyg3 with

HindIII. New mutants will be transformed with a PCR product that contains only the hygromycin resistance gene, but lacks the promoter.

Mutant Screening

Mutants were grown in 15 mL of TAP media for two days or until light to medium green. They were then screened based on their ability to phototax by using a box in which test tubes of culture were incubated for 4 minutes so that only a slit of light shone through to the sample. The tubes were then observed to have a distinct green line where the slit of light was if they are phototaxis positive, and these strains were discarded. Phototaxis negative strains had no distinct line and either had media that was homogenously green or had cells sink to the bottom, making the bottom of the tube more green (**Figure 10**). If strains were bald, they tended to have cells that clumped and this was visible with the naked eye. All strains that could not swim toward the light were kept for further screening.

Cells were then observed under a compound light microscope to determine if they had visible flagellar or motility abnormalities and were categorized based on phenotype. Lugol's iodine was used to fix cells to observe the flagella of cells that were motile.

Western blot analysis revealed whether or not there were differences in expression of IFT or motor proteins to further screen for strains likely to have mutations in IFT-related genes. For detailed methods used to perform western blots, see methods in Chapter II (page 16). Antibodies used were against *Chlamydomonas reinhardtii* IFT139 [9], IFT80, IFT46 [27], and FLA10 [9].

DNA Extraction

For a quick extraction of DNA from each of the mutants, the following protocol was followed:

1. Scrape a small amount of *Chlamydomonas reinhardtii* cells from a fresh plate with a sterile yellow micropipette tip or toothpick and resuspend in 20 µl H_2O in a microcentrifuge tube.
2. Add 20 µl 100% ethanol
3. Mix well by pipetting up and down
4. Add 200 µl 5% Chelex solution*
5. Boil for 10 minutes
6. Centrifuge at room temperature for 10 mins
7. Transfer the supernatant to a new tube to be used for PCR (use 1µl per PCR reaction)
8. Store at -20ºC for short term or -80ºC for long term storage.

*Chelex preparation: 5% (w/v) in H_2O:

1. 5g Chelex® 100 Resin, add ddH_2O to 100 ml
2. Mix well using heat and stir bar (will not become clear)
3. Autoclave for 15 mins
4. pH should be greater than 9 for best results

Note: Chelex is insoluble, so be sure to swirl well before each use to ensure that the concentration of beads is correct.

RESDA PCR

Methods used for RESDA PCR are based, with some slight adjustments, on the protocol given to our lab by Jason Brown from the Witman lab. Three degenerate primers were used, and both ends of the insert were amplified so that each mutant had a total of six primary PCR reactions (**Tables 2 and 3**).

Table 2. RESDA Primary PCR Reaction	
Volume (µl)	**Reagent**
0.5	10µM Linearized Plasmid Primer
1.5	10µM Degenerate Primer
2.5	5X Green GoTaq® Reaction Buffer (Promega)
0.125	GoTaq® DNA Polymerase (Promega)
0.2	10 mM dNTPs
0.375	DMSO
0.5	25 mM $MgCl_2$
6.3	ddH_2O
0.5	Mutant DNA (about 50 ng/µl)

Table 3. RESDA Primary PCR Program		
Step	**Temperature (ºC)**	**Time (min)**
1	95	2
2	94	1
3	62	1
4	72	2.5
5	Repeat steps 2-4 4X	
6	94	1
7	25	3
8	72 (Ramp rate: 0.3ºC/s)	2.5
9	94	.5
10	68	1
11	72	2.5
12	94	.5
13	68	1
14	72	2.5
15	94	.5
16	44	1
17	72	2.5
18	Repeat steps 9-17 14X	
19	72	5
20	Hold at 16	∞

A secondary PCR reaction was then used to increase the specificity of the primary RESDA PCR product (**Tables 4 and 5**).

Table 4. RESDA Secondary PCR Reaction	
Volume (µl)	**Reagent**
0.5	10µM Linearized Plasmid Primer
0.5	10µM Degenerate Primer
2.5	5X Green GoTaq® Reaction Buffer (Promega)
0.125	GoTaq® DNA Polymerase (Promega)
0.2	10 mM dNTPs
0.375	DMSO
0.5	25 mM $MgCl_2$
7.3	ddH_2O
0.5	Mutant DNA (primary PCR product diluted 1:25)

Table 5. RESDA Secondary PCR Program		
Step	**Temperature (ºC)**	**Time (min)**
1	95	2
2	95	.5
3	60	.5
4	72	3
5	Repeat steps 2-4 34X	
6	72	10
7	Hold at 16	∞

Primers

The Q0 primer and degenerate primers with restriction enzyme sites and Q0 were based on methods in Gonzalez-Ballester, *et al*, 2005 [30]. DegAluI was not used. Primer sequences used for the ends of the inserts in mutants created using pHyg3 digested with

HindIII were DP3, DP4, UP1 (Labeled UP_1 in **Fig. 14**), and UP2 from methods in Matsuo, *et al*, 2008 [49]. All other primers were designed using Primer3 (**Table 6**).

Table 6. Primers Designed for RESDA PCR		
5' end right primers of pHyg3 cut with *ScaI*	Up3	ATT GCT ACA GGC ATC GTG GT
	Up4	GCA GAA GTG GTC CTG CAA CT
	Up5	TCG TCG TTT GGT ATG GCT TC
3’ end left primers of pHyg3cut with *ScaI*	Dwn1	GCG CGG AAC CCC TAT TTG TTT A
	Dwn2	CCG CTC ATG AGA CAA TAA CCC TGA
Primer to check for specificity of Up primers	SpecU	CAT GGG GGA TCA TGT AAC TC
	SpecU2	GCG GCC AAC TTA CTT CTG AC
Other primers used	Dwn3	GCC TGA TGC GGT ATT TTC TC
	IFT80F	GTC AGC ACT CTG GAC GCA TA
	IFT80U	GAC TTG ATG ACC ACG TTG GA
	IFT80D	GTA CTC CAC CCA GCA CAC CT
	PF16UP	GAA CAT GTT GCT GGC ACT TAG TCA CG
	PF16DP	GGC GGT GGC GCT TTT GAG GTG G

Sequencing

Standard sequencing was performed by Eurofins Scientific. Phytozome v8.0 from www.chlamy.org, NCBI BLAST, and Sequencher software were used for sequence analysis and identification of the disrupted gene.

CHAPTER V

SUMMARY AND CONCLUSIONS

This study dissected the roles that IFT B proteins play on the stability, assembly, and localization of complex B. Sucrose density gradients and cycloheximide time-course treatments revealed that IFT52 is required for the stability and assembly of the core complex B (**Figs. 4E and 3D, E**), while IFT46 is not required for the assembly of the core (**Fig. 3B**) but is necessary to maintain stability of the complex (**Fig. 4D)**. This explains why *bld1*is unable to perform ciliogenesis having a bald phenotype (**Fig. 2**), yet *ift46* can produce flagella but they are severely shortened (**Fig. 2**) due to the complex's lack of stability and fast turnover rate. IFT88, although a part of the core complex B, is necessary for neither the assembly nor the stability of complex B (**Figs. 3C and 4C**). Sucrose density gradients showed that in *ift88* all core proteins cosedimented to form an intact, but slightly smaller complex (**Fig. 3C**), showing that IFT88 is not necessary to build the core but is probably required to bind peripheral proteins to the core. *Ift88*'s lack of flagella can be explained by the immunofluorescent stains that show IFT particle B fails to localize to the apical end of the basal body. This means that even though the core complex B is intact, it is missing a component necessary to localize to the initiation site for ciliogenesis, causing a bald phenotype. It is yet to be determined whether it is IFT80 itself, or if it is one of the proteins that is bridged by IFT80 to the core complex B, that is

essential for the proper localization of complex B. Null mutants, RNAi, or microRNA knockdowns of peripheral proteins would help answer this question. The results of this study are explained by a model in which complex B is sequentially assembled, by first assembling the core which then binds to peripheral proteins and is next localized to the apical end of the basal body to initiate ciliogenesis (**Fig. 8**).

Little is known about the functions or interactions of peripheral proteins. Yeast two-hybrid analysis will be used to further investigate protein-protein interactions between core and peripheral proteins and among peripheral proteins. This will build on our knowledge of the architecture of complex B and how peripheral proteins interact with the core to permit IFT to take place in order to build flagella.

In an attempt to obtain new null mutants for peripheral IFT B proteins, random insertional mutagenesis was employed. To screen these for IFT mutants, only phototaxis negative mutants with defective flagella were investigated. RESDA PCR is proving to be useful in identifying the disrupted genes in these mutants. So far, five interesting flagella-related mutants have been identified, three of these being strains with disrupted *IFT80*, *PF16*, and *CEP290*. However, all of these genes already have mutants available to the scientific community, so they have not been confirmed or pursued. RESDA will be continued on our growing library of mutants in hopes that many more IFT mutants, preferably one null for an IFT B peripheral protein, will be identified.

Once novel mutants are discovered through the screening process, they will be backcrossed and confirmed by rescuing their phenotypes. Once the mutation is confirmed, we will engage in an in-depth phenotypic analysis. Cells will be examined in

detail microscopically to determine the morphology of the strain. Sucrose density gradients and cycloheximide treatments will show the protein's effect on assembly and stability, respectively, of complex B. Immunofluorescent staining will show if the mutation causes a defect in localization patterns of IFT particles. In mutants that still have flagella, it may be useful to investigate if there is a disruption in important flagella-related pathways such as the hedgehog signaling pathway. It is important to continue this mutant screen through RESDA PCR because novel mutants will be great tools to build our continually growing knowledge of the IFT process and its role in ciliogenesis.

REFERENCES

1. Hildebrandt F, Benzing T, Katsanis N (2011) Ciliopathies. N Engl J Med 364: 1533-1543.

2. Ishikawa H, Marshall WF (2011) Ciliogenesis: building the cell's antenna. Nat Rev Mol Cell Biol 12: 222-234.

3. Pigino G, Geimer S, Lanzavecchia S, Paccagnini E, Cantele F, et al. (2009) Electron-tomographic analysis of intraflagellar transport particle trains in situ. J Cell Biol 187: 135-148.

4. Mukhopadhyay S, Wen X, Chih B, Nelson CD, Lane WS, et al. (2010) TULP3 bridges the IFT-A complex and membrane phosphoinositides to promote trafficking of G protein-coupled receptors into primary cilia. Genes Dev 24: 2180-2193.

5. Iomini C, Li L, Esparza JM, Dutcher SK (2009) Retrograde intraflagellar transport mutants identify complex A proteins with multiple genetic interactions in *Chlamydomonas reinhardtii*. Genetics 183: 885-896.

6. Cole DG (2003) The intraflagellar transport machinery of *Chlamydomonas reinhardtii*. Traffic 4: 435-442.

7. Williamson, S., Silva, D., Richey, E., and Qin, H. (2012). Probing the role of IFT particle complex A and B in flagellar entry and exit of IFT-dynein in *Chlamydomonas*. Protoplasma 249, 851-856.

8. Tran PV, Haycraft CJ, Besschetnova TY, Turbe-Doan A, Stottmann RW, et al. (2008) THM1 negatively modulates mouse sonic hedgehog signal transduction and affects retrograde intraflagellar transport in cilia. Nat Genet 40: 403-410.

9. Cole DG, Diener DR, Himelblau AL, Beech PL, Fuster JC, et al. (1998) *Chlamydomonas* kinesin-II-dependent intraflagellar transport (IFT): IFT particles contain proteins required for ciliary assembly in *Caenorhabditis elegans* sensory neurons. J Cell Biol 141: 993-1008.

10. Piperno G, Mead K (1997) Transport of a novel complex in the cytoplasmic matrix of *Chlamydomonas* flagella. Proc Natl Acad Sci U S A 94: 4457-4462.

11. Behal RH, Miller MS, Qin H, Lucker BF, Jones A, et al. (2012) Subunit interactions and organization of the *Chlamydomonas reinhardtii* intraflagellar transport complex A proteins. J Biol Chem 287: 11689-11703.

12. Lucker BF, Behal RH, Qin H, Siron LC, Taggart WD, et al. (2005) Characterization of the intraflagellar transport complex B core: direct interaction of the IFT81 and IFT74/72 subunits. J Biol Chem 280: 27688-27696.

13. Taschner M, Bhogaraju S, Vetter M, Morawetz M, Lorentzen E (2011) Biochemical mapping of interactions within the intraflagellar transport (IFT) B core complex: IFT52 binds directly to four other IFT-B subunits. J Biol Chem 286: 26344-26352.

14. Wang Z, Fan ZC, Williamson SM, Qin H (2009) Intraflagellar transport (IFT) protein IFT25 is a phosphoprotein component of IFT complex B and physically interacts with IFT27 in *Chlamydomonas*. PLoS One 4: e5384.

15. Bhogaraju S, Taschner M, Morawetz M, Basquin C, Lorentzen E (2011) Crystal structure of the intraflagellar transport complex 25/27. EMBO J 30: 1907-1918.

16. Lucker BF, Miller MS, Dziedzic SA, Blackmarr PT, Cole DG (2010) Direct interactions of intraflagellar transport complex B proteins IFT88, IFT52 and IFT46. J Biol Chem 2010.

17. Fan ZC, Behal RH, Geimer S, Wang ZH, Williamson SM, et al. (2010) *Chlamydomonas* IFT70/CrDYF-1 is a core component of IFT particle complex B and is required for flagellar assembly. Molecular Biology of the Cell 21: 2696-2706.

18. Perkins LA, Hedgecock EM, Thomson JN, Culotti JG (1986) Mutant sensory cilia in the nematode *Caenorhabditis elegans*. Dev Biol 117: 456-487.

19. Bell LR, Stone S, Yochem J, Shaw JE, Herman RK (2006) The molecular identities of the *Caenorhabditis elegans* intraflagellar transport genes dyf-6, daf-10 and osm-1. Genetics 173: 1275-1286.

20. Ou G, Blacque OE, Snow JJ, Leroux MR, Scholey JM (2005) Functional coordination of intraflagellar transport motors. Nature 436: 583-587.

21. Hao L, Thein M, Brust-Mascher I, Civelekoglu-Scholey G, Lu Y, et al. (2011) Intraflagellar transport delivers tubulin isotypes to sensory cilium middle and distal segments. Nat Cell Biol 13: 790-798.

22. Kobayashi T, Gengyo-Ando K, Ishihara T, Katsura I, Mitani S (2007) IFT-81 and IFT-74 are required for intraflagellar transport in *C. elegans*. Genes Cells 12: 593-602.

23. Pazour GJ, Dickert BL, Vucica Y, Seeley ES, Rosenbaum JL, et al. (2000) *Chlamydomonas* IFT88 and its mouse homologue, polycystic kidney disease gene tg737, are required for assembly of cilia and flagella. J Cell Biol 151: 709-718.

24. Han YG, Kwok BH, Kernan MJ (2003) Intraflagellar transport is required in *Drosophila* to differentiate sensory cilia but not sperm. Curr Biol 13: 1679-1686.

25. Murcia NS, Richards WG, Yoder BK, Mucenski ML, Dunlap JR, et al. (2000) The Oak Ridge Polycystic Kidney (orpk) disease gene is required for left-right axis determination. Development 127: 2347-2355.

26. Brazelton WJ, Amundsen CD, Silflow CD, Lefebvre PA (2001) The *bld1* mutation identifies the *Chlamydomonas* osm-6 homolog as a gene required for flagellar assembly. Curr Biol 11: 1591-1594.

27. Hou Y, Qin H, Follit JA, Pazour GJ, Rosenbaum JL, et al. (2007) Functional analysis of an individual IFT protein: IFT46 is required for transport of outer dynein arms into flagella. J Cell Biol 176: 653-665.

28. Dave D, Wloga D, Sharma N, Gaertig J (2009) DYF-1 Is required for assembly of the axoneme in Tetrahymena thermophila. Eukaryot Cell 8: 1397-1406.

29. Chien CT, Bartel PL, Sternglanz R, Fields S (1991) The two-hybrid system: a method to identify and clone genes for proteins that interact with a protein of interest. Proc Natl Acad Sci U S A 88: 9578-9582.

30. Gonzalez-Ballester D, de Montaigu A, Galvan A, Fernandez E (2005) Restriction enzyme site-directed amplification PCR: a tool to identify regions flanking a marker DNA. Anal Biochem 340: 330-335.

31. Pedersen LB, Miller MS, Geimer S, Leitch JM, Rosenbaum JL, et al. (2005) *Chlamydomonas* IFT172 is encoded by FLA11, interacts with CrEB1, and regulates IFT at the flagellar tip. Curr Biol 15: 262-266.

32. Bhogaraju S, Taschner M, Morawetz M, Basquin C, Lorentzen E (2011) Crystal structure of the intraflagellar transport complex 25/27. EMBO J 30, 1907-1918.

33. Silva DA, Huang X, Behal RH, Cole DG, Qin H (2012) The RABL5 homolog IFT22 regulates the cellular pool size and the amount of IFT particles partitioned to the flagellar compartment in *Chlamydomonas reinhardtii*. Cytoskeleton (Hoboken) 69: 33-48.

34. Qin H, Wang Z, Diener D, Rosenbaum J (2007) Intraflagellar transport protein 27 is a small G protein involved in cell-cycle control. Curr Biol 17: 193-202.

35. Scholey JM (2008) Intraflagellar transport motors in cilia: moving along the cell's antenna. J Cell Biol 180: 23-29.

36. Kozminski KG, Beech PL, Rosenbaum JL (1995) The *Chlamydomonas* kinesin-like protein FLA10 is involved in motility associated with the flagellar membrane. J Cell Biol 131: 1517-1527.

37. Mueller J, Perrone CA, Bower R, Cole DG, Porter ME (2005) The FLA3 KAP subunit is required for localization of kinesin-2 to the site of flagellar assembly and processive anterograde intraflagellar transport. Mol Biol Cell 16: 1341-1354.

38. Deane JA, Cole DG, Seeley ES, Diener DR, Rosenbaum JL (2001) Localization of intraflagellar transport protein IFT52 identifies basal body transitional fibers as the docking site for IFT particles. Curr Biol 11: 1586-1590.

39. Baker SA, Freeman K, Luby-Phelps K, Pazour GJ, Besharse JC (2003) IFT20 links kinesin II with a mammalian intraflagellar transport complex that is conserved in motile flagella and sensory cilia. J Biol Chem 278: 34211-34218.

40. Dutcher SK, Li L, Lin H, Meyer L, Giddings TH, Jr., et al. (2012) Whole-genome sequencing to identify mutants and polymorphisms in *Chlamydomonas reinhardtii*. G3 (Bethesda) 2: 15-22.

41. Engel BD, Ludington WB, Marshall WF (2009) Intraflagellar transport particle size scales inversely with flagellar length: revisiting the balance-point length control model. J Cell Biol 187: 81-89.

42. Snow JJ, Ou G, Gunnarson AL, Walker MR, Zhou HM, et al. (2004) Two anterograde intraflagellar transport motors cooperate to build sensory cilia on *C. elegans* neurons. Nat Cell Biol 6: 1109-1113.

43. Qin H, Diener DR, Geimer S, Cole DG, Rosenbaum JL (2004) Intraflagellar transport (IFT) cargo: IFT transports flagellar precursors to the tip and turnover products to the cell body. J Cell Biol 164: 255-266.

44. Beales PL, Bland E, Tobin JL, Bacchelli C, Tuysuz B, et al. (2007) IFT80, which encodes a conserved intraflagellar transport protein, is mutated in Jeune asphyxiating thoracic dystrophy. Nat Genet 39: 727-729.

45. Rix S, Calmont A, Scambler PJ, Beales PL (2011) An *Ift80* mouse model of short rib polydactyly syndromes shows defects in hedgehog signalling without loss or malformation of cilia. Hum Mol Genet 20: 1306-1314.

46. Smith EF, Lefebvre PA (1996) PF16 encodes a protein with armadillo repeats and localizes to a single microtubule of the central apparatus in *Chlamydomonas* flagella. J Cell Biol 132: 359-370.

47. Craige B, Tsao CC, Diener DR, Hou Y, Lechtreck KF, et al. (2010) CEP290 tethers flagellar transition zone microtubules to the membrane and regulates flagellar protein content. J Cell Biol 190: 927-940.

48. Berthold P, Schmitt R, Mages W (2002) An engineered Streptomyces hygroscopicus aph 7" gene mediates dominant resistance against hygromycin B in *Chlamydomonas reinhardtii*. Protist 153: 401-412.

49. Matsuo T, Okamoto K, Onai K, Niwa Y, Shimogawara K, et al. (2008) A systematic forward genetic analysis identified components of the *Chlamydomonas* circadian system. Genes & Development 22: 918-930.